Report

Current Biology

Alkaloids are associated with increased microbial diversity and metabolic function in poison frogs

Graphical abstract

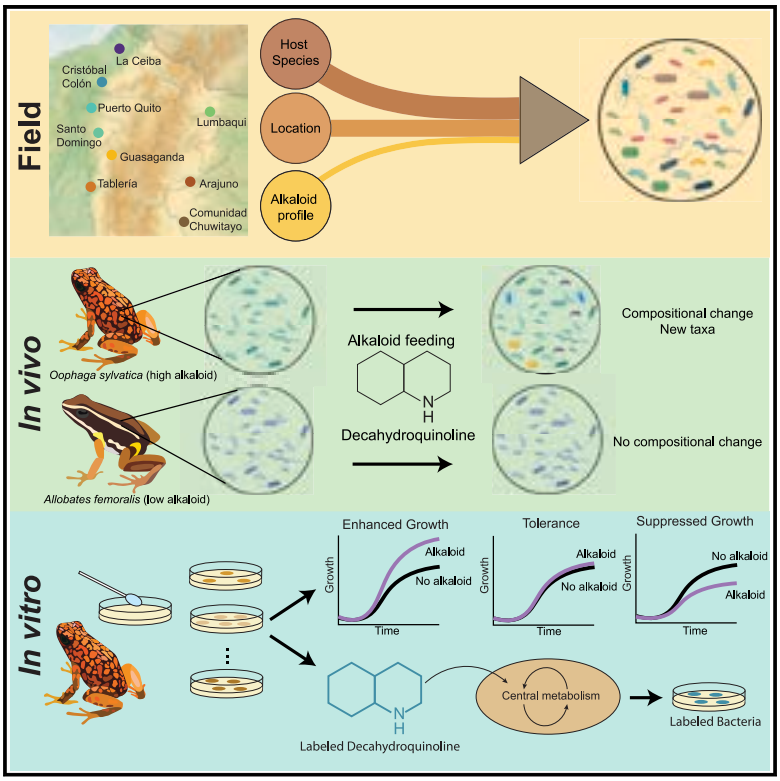

Highlights

- Host species, location, and alkaloid quantity influence poison frog skin microbiomes
- Alkaloid exposure impacts microbiomes of high- and low-alkaloid frogs differently
- Bacterial strains from a poison frog can metabolize the alkaloid decahydroquinoline

Authors

Stephanie N. Caty, Aurora Alvarez-Buylla, Cooper Vasek, ..., Luis A. Coloma, Megan M. Morris, Lauren A. O'Connell

Correspondence

scaty@stanford.edu (S.N.C.), loconnel@stanford.edu (L.A.O.)

In brief

Caty et al. demonstrate that alkaloids play a role in structuring the skin microbial community of dendrobatid poison frogs. They provide evidence that this is partly due to the ability of some microbial taxa to metabolize alkaloids.

Caty et al., 2025, Current Biology *35*, 1–11
January 6, 2025
https://doi.org/10.1016/j.cub.2024.10.069

CellPress

Please cite this article in press as: Caty et al., Alkaloids are associated with increased microbial diversity and metabolic function in poison frogs, Current Biology (2024), https://doi.org/10.1016/j.cub.2024.10.069

Current Biology

CellPress

Report

Alkaloids are associated with increased microbial diversity and metabolic function in poison frogs

Stephanie N. Caty,[1,7,*] Aurora Alvarez-Buylla,[1] Cooper Vasek,[1] Elicio E. Tapia,[2] Nora A. Martin,[1] Theresa McLaughlin,[3] Chloe L. Golde,[1] Peter K. Weber,[4] Xavier Mayali,[4] Luis A. Coloma,[5] Megan M. Morris,[4] and Lauren A. O'Connell[1,6,8,9,*]

[1]Department of Biology, Stanford University, Stanford, CA 94305, USA
[2]Leibniz Institute for the Analysis of Biodiversity Change, Martin-Luther-King-Platz 3, Hamburg 20146, Germany
[3]Stanford University Mass Spectrometry, Stanford University, Stanford, CA 94305, USA
[4]Physical and Life Sciences Directorate, Lawrence Livermore National Laboratory, Livermore, CA 94550, USA
[5]Centro Jambatu de Investigación y Conservación de Anfibios, Fundación Jambatu, San Rafael, Quito 170810, Ecuador
[6]Sarafan ChEM-H, Stanford University, Stanford, CA 94305, USA
[7]X (formerly Twitter): @stephaniecaty
[8]X (formerly Twitter): @LOB_SU
[9]Lead contact
*Correspondence: scaty@stanford.edu (S.N.C.), loconnel@stanford.edu (L.A.O.)
https://doi.org/10.1016/j.cub.2024.10.069

SUMMARY

Shifts in host-associated microbiomes can impact both host and microbes.[1–6] It is of interest to understand how perturbations, like the introduction of exogenous chemicals,[7–13] impact microbiomes. In poison frogs (family Dendrobatidae), the skin microbiome is exposed to alkaloids that the frogs sequester for defense.[14–19] These alkaloids are antimicrobial[20–22]; however, their effect on the frogs' skin microbiome is unknown. To test this, we characterized microbial communities from field-collected dendrobatid frogs. Then, we conducted a laboratory experiment to monitor the effect of the alkaloid decahydroquinoline (DHQ) on the microbiome of two frog species with contrasting alkaloid loads in nature. In both datasets, we found that alkaloid-exposed microbiomes were more phylogenetically diverse, with an increase in diversity among rare taxa. To better understand the isolate-specific response to alkaloids, we cultured microbial isolates from poison frog skin and found that many isolates exhibited enhanced growth or were not impacted by the addition of DHQ. To further explore the microbial response to alkaloids, we sequenced the metagenomes from high- and low-alkaloid frogs and observed a greater diversity of genes associated with nitrogen and carbon metabolism in high-alkaloid frogs. From these data, we hypothesized that some strains may metabolize the alkaloids. We used stable isotope tracing coupled to nanoSIMS (nanoscale secondary ion mass spectrometry), which supported the idea that some of these isolates are able to metabolize DHQ. Together, these data suggest that poison frog alkaloids open new niches for skin-associated microbes with specific adaptations, such as alkaloid metabolism, that enable survival in this environment.

RESULTS

Alkaloids increased microbial community diversity, while host species and location correlated with overall composition

We characterized the bacterial and fungal communities of frog skins from 11 species of frogs across nine geographic locations in Ecuador (Figure 1A; Table S1). For some alkaloid comparisons, the frogs were grouped into three categories of summed alkaloid load, as defined by the summed area under the curve of all alkaloids: high, medium, and low alkaloids (Kruskal-Wallis chi-squared = 127.66, df = 2, $p < 0.001$, post hoc Dunn Kruskal-Wallis multiple comparison $p < 0.001$ for all pairwise comparisons; Figure 1B). The phylogeny of the host species and the location of collection were significantly correlated with the bacterial community composition, whereas the composition of the alkaloid profiles was not (Figure 1C, Mantel tests: phylogeny R = 0.12, $p = 0.001$; location R = 0.07, $p = 0.04$, alkaloids R = 0.004, $p = 0.5$). The phylogenetic correlation persisted in a partial Mantel test to account for location (R = 0.11, $p = 0.003$). A PERMANOVA analysis on Bray-Curtis dissimilarity found that location ($R^2 = 0.25$, $F_{(9, 204)} = 7.64$, $p = 0.001$), host species ($R^2 = 0.07$, $F_{(9, 204)} = 2.32$, $p = 0.001$), and their interaction ($R^2 = 0.02$, $F_{(3, 204)} = 2.27$, $p = 0.001$) were statistically significant.

Unlike taxonomic composition, bacterial diversity from the frog skin was related to host alkaloid levels. Specifically, high-alkaloid frogs had a greater number of bacterial amplicon sequence variants (ASVs) than low-alkaloid frogs (Figure 1D, upper panel, $F_{(2, 202)} = 7.2$, $p = 0.0009$, high vs. low alkaloids $p = 0.0007$). Furthermore, the phylogenetic diversity (Faith's phylogenetic diversity) was higher in high-alkaloid frogs than in either medium-alkaloid or low-alkaloid frogs (Figure 1D, lower panel, $F_{(2, 202)} = 7.6$, $p = 0.0006$, high vs. low $p = 0.03$, high vs. no $p = 0.0006$). To characterize the taxa driving these differences, we used the R package

Please cite this article in press as: Caty et al., Alkaloids are associated with increased microbial diversity and metabolic function in poison frogs, Current Biology (2024), https://doi.org/10.1016/j.cub.2024.10.069

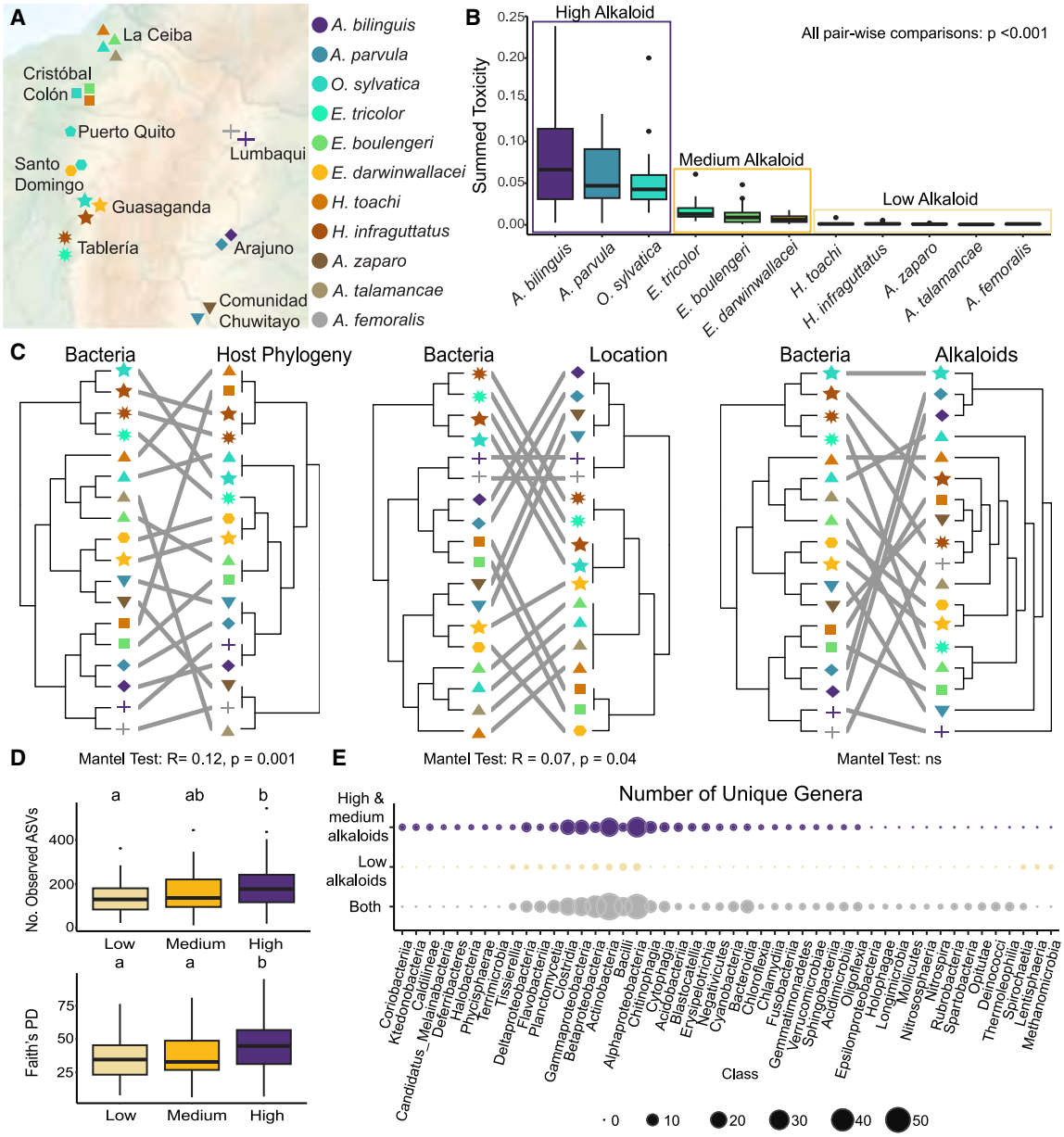

Figure 1. Host species and collection location influence bacterial composition; alkaloids increase diversity

(A) Eleven species of frogs (color) were collected from nine locations (shape) in Ecuador.

(B) Based on summed alkaloid content, frog species can be grouped into those with high, medium, and low alkaloids. Using a Kruskal-Wallace and post hoc Dunn's test, pairwise comparisons between groups have $p < 0.001$, boxplots denote median with interquartile range (IQR) ± 1.5*IQR, dots are outlier points.

(C) Bacterial communities are correlated with host phylogeny (Mantel test R = 0.12, $p = 0.001$) and geographic location (Mantel test R = 0.07, $p = 0.04$).

(D) Bacterial communities from high-alkaloid frogs are more speciose and more phylogenetically diverse (PD, phylogenetic diversity) than frogs with low alkaloids. Letters denote statistical differences based on Dunn's post hoc test with $p < 0.05$, boxplots denote median with IQR ± 1.5*IQR, dots are outlier points.

(E) The number of unique bacterial genera found in frogs with high or medium alkaloids is greater than those found only in those with low alkaloids, based on ANCOMBC structural zeroes. Frog species: *Ameerega bilinguis*, *Ameerega parvula*, *Oophaga sylvatica*, *Epipedobates tricolor*, *Epipedobates boulengeri*, *Epipedobates darwinwallacei*, *Hyloxalus toachi*, *Hyloxalus infraguttatus*, *Allobates zaparo*, *Allobates talamancae*, and *Allobates femoralis*.

See also Figure S1 and Tables S1 and S2.

ANCOMBC[23] to create a presence/absence comparison of genera across groups. When comparing higher-alkaloid-containing frogs (high and medium) to low-alkaloid frogs, 154 bacterial genera were present only in higher alkaloid frogs and 19 bacterial genera were present only in low-alkaloid frogs (Figure 1E; Table S2). These higher alkaloid taxa comprised 5% of the total bacterial communities of higher alkaloid frogs, suggesting that some of these differences in diversity were attributed to the presence of low-abundance taxa. We observed similar patterns of increased diversity associated with alkaloid presence for fungal communities

Please cite this article in press as: Caty et al., Alkaloids are associated with increased microbial diversity and metabolic function in poison frogs, Current Biology (2024), https://doi.org/10.1016/j.cub.2024.10.069

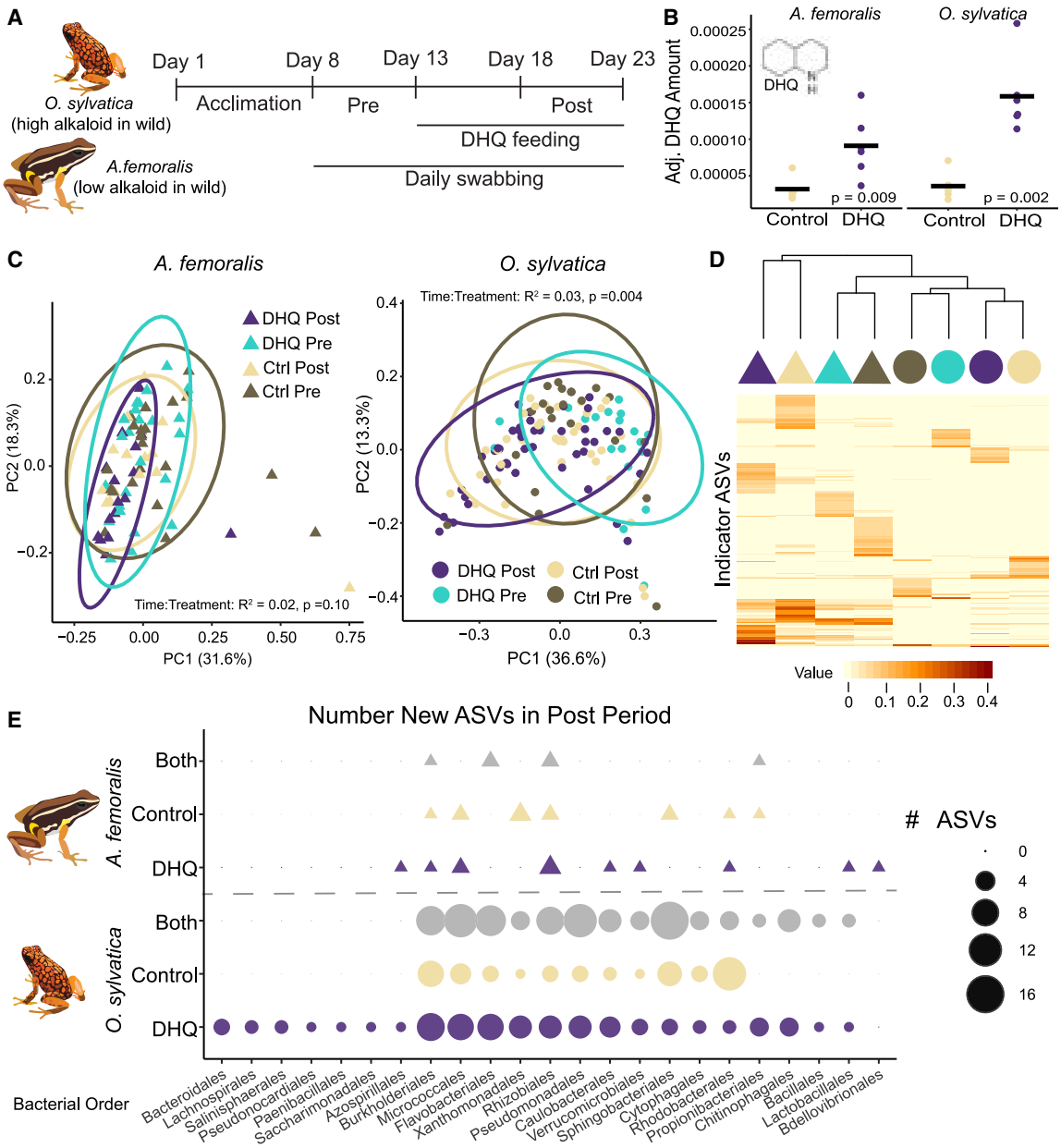

Figure 2. Bacterial communities responded differently to an alkaloid in OS and AF

(A) Feeding experiment overview.

(B) Quantification of DHQ showed accumulation in DHQ-fed frogs, but not in control frogs, in both OS and AF.

(C) Based on weighted UniFrac distance, DHQ treatment elicited a differential response over time compared with control frogs in OS but not in AF.

(D) Indicator ASVs (based on frequency and abundance) grouped samples primarily by frog species and secondarily by experimental time point (pre vs. post).

(E) The number of new ASVs from unique orders in the post-treatment period was greatest for DHQ-fed OS frogs.

See also Figure S2 and Table S3.

(Figure S1; Table S2). Notably the genus containing the fungal pathogen *Batrachochytrium dendrobatidis* was less abundant in higher-alkaloid-containing frogs (Figure S1E).

A single alkaloid changed the resident skin microbial community

To test the hypothesis that alkaloids shift microbial communities and remove the confounding factors of environment and host species, we performed controlled lab toxin feeding experiments with two species from our field data: the high-alkaloid Diablito poison frog (*Oophaga sylvatica*, hereafter OS) and the low-alkaloid brilliant-thighed poison frog (*Allobates femoralis*, hereafter AF). Frogs were swabbed for 5 days prior to alkaloid administration and for the 10 days of administration of the experimental treatment using either decahydroquinoline (DHQ) or vehicle control (water) (Figure 2A). DHQ was selected as it is commonly

Please cite this article in press as: Caty et al., Alkaloids are associated with increased microbial diversity and metabolic function in poison frogs, Current Biology (2024), https://doi.org/10.1016/j.cub.2024.10.069

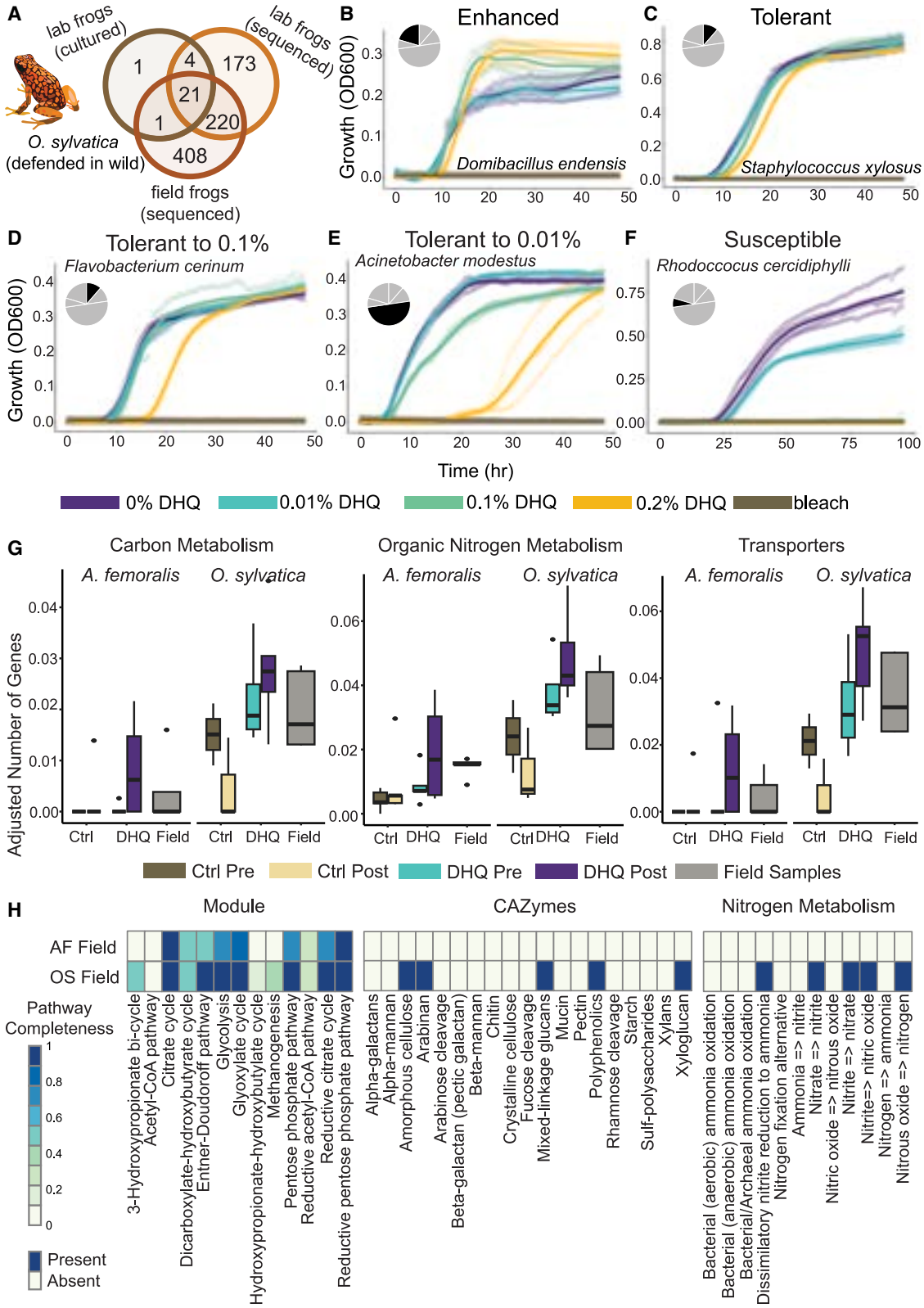

Figure 3. Bacterial isolates vary in response when grown in DHQ, which may reflect differences in metabolic capabilities

(A–F) (A) Overlap in bacterial taxa found in the lab, field, and cultures from *Oophaga sylvatica* (OS). Growth patterns of isolates were categorized into those that exhibit enhanced growth with DHQ (B; 20%), those that were tolerant to all tested concentrations (C; 11%), those that were tolerant up to 0.1% DHQ (D; 11%),

(legend continued on next page)

Please cite this article in press as: Caty et al., Alkaloids are associated with increased microbial diversity and metabolic function in poison frogs, Current Biology (2024), https://doi.org/10.1016/j.cub.2024.10.069

found on poison frogs in the wild and is commercially available. Swabs were used for characterization of the bacterial and fungal communities. At the end of the feeding experiment, frog skins were used to quantify alkaloid load. As expected, the OS fed DHQ sequestered the DHQ onto their skin, whereas control frogs did not (Figure 2B, Wilcoxon rank sum test W = 0, $p = 0.004$). Unexpectedly, the AF also sequestered DHQ onto their skin (Figure 2B, Wilcoxon rank sum test W = 1, $p = 0.009$).

The bacterial compositional changes over time were different between the treatment groups in OS but not in AF (Figure 2C, OS time $R^2 = 0.06$, $F_{(1, 122)} = 9.02$, $p = 0.001$; time:treatment $R^2 = 0.03$, $F_{(1, 122)} = 3.8$, $p = 0.006$, AF time $R^2 = 0.04$, $F_{(1, 75)} = 3.05$, $p = 0.005$; time:treatment $R^2 = 0.02$, $F_{(1, 75)} = 1.644$, $p = 0.12$). Clustering of bacterial communities based on indicator ASVs, identified based on frequency and abundance within each group, found that frog species was the primary axis of grouping and that the experimental time frame (pre vs. post treatment exposure) was a more significant driver of taxa composition than treatment (Figure 2D).

Structural zeroes were identified using ANCOMBC to identify bacterial taxa that arose in the post time period (Figure 2E; Table S3). Within OS, 132 new ASVs appeared in both treatment groups, 79 appeared in only DHQ-fed frogs, and 54 appeared in control frogs. Within AF, 8 new ASVs arose in both treatments, 13 in DHQ-fed and 14 in control frogs. Although there was substantial overlap between new ASVs across the frog species, many of the ASVs that appeared in DHQ-fed OS were not seen in any other groups, including 10 from bacterial orders not detected in any of the other groups. Unlike the bacteria, the fungal community composition did not change within either species. However, the fungal community diversity did decrease in DHQ-fed AF (Figure S2; Table S3).

Differential responses to alkaloids suggest increased metabolic diversity in OS microbes

We next tested how individual bacterial and fungal isolates responded to the presence of an individual alkaloid, DHQ. We generated 132 isolates (27 genera and 45 species) from OS. Of these 27 genera, 21 were found in amplicon-sequencing data from both the lab frogs and wild frogs (Figure 3A), and, together, these genera comprise, on average, 66% and 30% of total bacterial communities of lab and field frogs, respectively. Using one isolate per species, based on the closest full-length 16S rRNA gene BLAST match, we quantified the growth of these isolates in increasing DHQ concentrations (0%, 0.01%, 0.1%, 0.2%, 1% w/v). Average area under the curve was calculated across four replicates per treatment. As was expected, no strains grew at 1% DHQ. Strains were subsequently categorized as having enhanced growth (20% of isolates; Figure 3B), full tolerance to DHQ (11%, Figure 3C), some amount of tolerance for DHQ (tolerant up to 0.1%: 11%, Figure 3D, tolerant to 0.01%: 49%, Figure 3E), or total susceptibility to DHQ (7%) (Figure 3F; Table S4). One strain did not fit into this categorization, as growth was impeded by 0.1% but not at 0.01% or at 0.2% DHQ. To explore the responses to alkaloids further, we sequenced metagenomes from wild AF and OS and from samples from both species in the feeding experiment. Using distilled and refined annotation of metabolism (DRAM) annotations, we categorized the number of unique genes, adjusted for the total number of genes identified in each assembly, into the following groups: carbon metabolism, organic nitrogen metabolism, and transporters. Metagenomes from OS frogs had a significantly higher number of genes associated with carbon and nitrogen metabolism, as well as cellular transport (Figure 3G). This was true when comparing all frogs together (nitrogen: $F_{(1, 41)} = 31.55$, $p < 0.001$; carbon: $F_{(1, 41)} = 37.14$, $p < 0.001$; transporters: $F_{(1, 41)} = 34.85$, $p < 0.001$), just the field frogs to each other (nitrogen: $F_{(1, 8)} = 7.83$, $p = 0.02$; carbon: $F_{(1, 8)} = 11.81$, $p = 0.009$; transporters: $F_{(1, 8)} = 24.67$, $p = 0.001$), or just the lab-reared frogs to each other (nitrogen: $F_{(1, 31)} = 23.6$, $p < 0.001$; carbon: $F_{(1, 31)} = 25.18$, $p < 0.001$; transporters: $F_{(1, 31)} = 19.89$, $p < 0.001$). We did not observe a significant difference in metabolic capabilities across treatments or time periods within the OS or AF feeding experiments. Assemblies from all wild frogs grouped together additionally showed greater metabolic functional diversity in OS than in AF across a variety of carbon- and nitrogen-based metabolic pathways (Figure 3H).

Some poison frog bacterial isolates can incorporate carbon from DHQ

To test whether there are microbes capable of metabolizing DHQ in the OS community, we swabbed a lab-reared OS and cultured that swab in liquid M9 minimal media with ^{13}C-labeled DHQ as the sole carbon source. Using nanoscale secondary ion mass spectrometry (nanoSIMS), the ^{13}C atom percent enrichment (APE) was measured to quantify uptake of ^{13}C from the labeled DHQ. We observed that some cells from the swab had higher enrichment of ^{13}C compared with the killed control cells or with natural ^{13}C abundance (Figure 4A). On average, the ^{13}C enrichment of cells from the swab was not higher than the killed controls; however, there was a subset of cells with very high enrichment (Figure 4B), suggesting that some cells cultured from the swab were able to utilize and incorporate ^{13}C from DHQ. To follow up on this, we selected two bacterial isolates that were isolated on media with DHQ as the sole carbon source, one from the genus *Providencia* and one from the genus *Serratia*, for additional isotope tracing experiments, this time using a reverse-labeling approach. The isolates were first grown in ^{13}C glucose to label the bacterial cells as much as possible and then transferred to media with a natural abundance of DHQ

those that were tolerant to 0.01% DHQ (E; 49%), and those that grew worse with any DHQ (F; 7%). Areas under the curve for all tested isolates can be found in Table S4.

(G) The adjusted number of genes attributed by DRAM annotation differs between the microbial communities of the frog species for carbon metabolism, nitrogen metabolism, and cellular transporters but does not vary significantly with treatment in the feeding experiment. Boxplots denote median with interquartile range (IQR) ± 1.5*IQR, dots are outlier points.

(H) OS frogs from the field have greater metabolic capabilities as compared with *Allobates femoralis* (AF), based on greater metabolic pathway completeness, more carbohydrate-active enzymes (CAZymes), and the presence of a greater diversity of nitrogen metabolic functions.

See also Table S4.

Please cite this article in press as: Caty et al., Alkaloids are associated with increased microbial diversity and metabolic function in poison frogs, Current Biology (2024), https://doi.org/10.1016/j.cub.2024.10.069

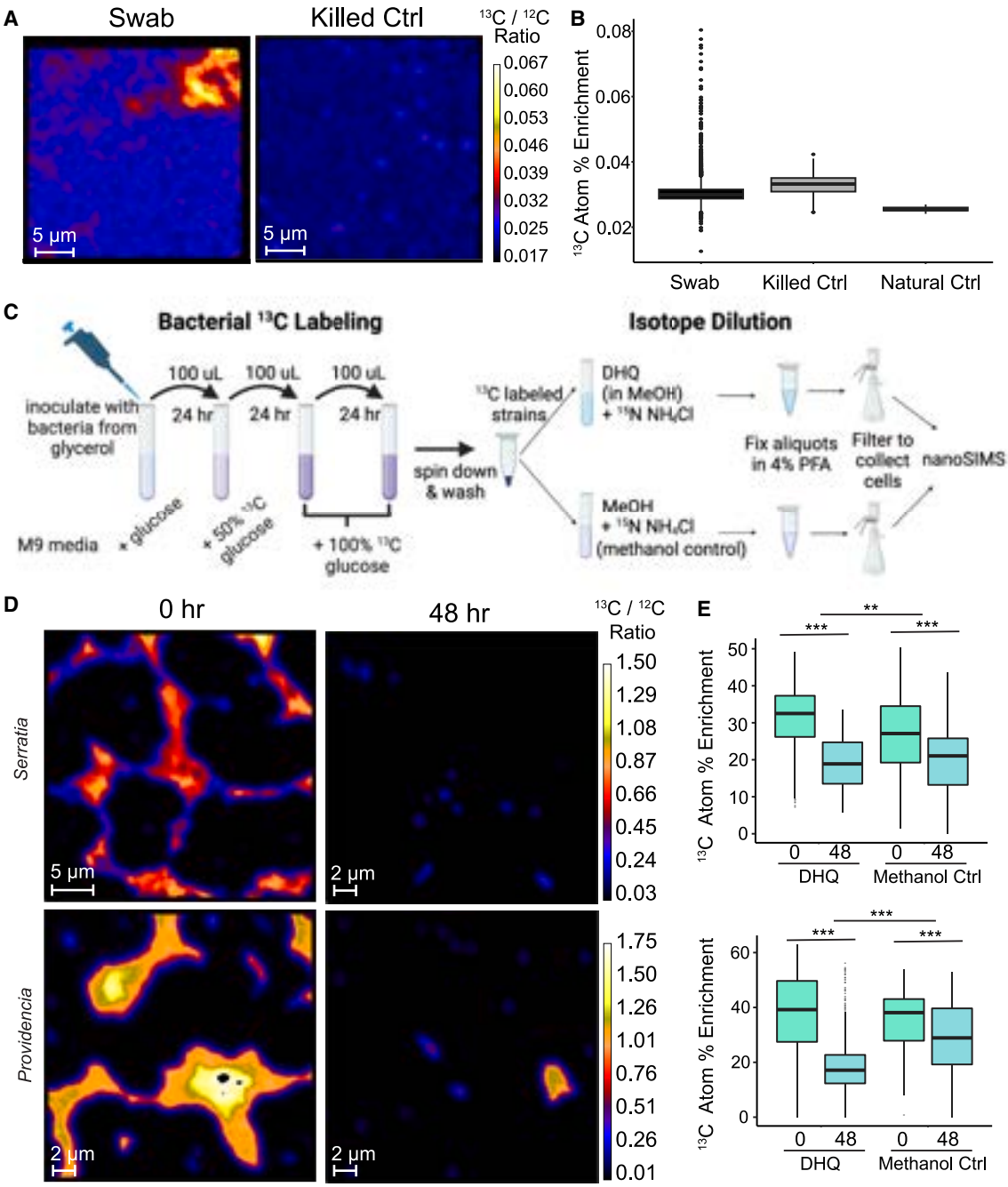

Figure 4. Isotope tracing suggests bacterial metabolism of an alkaloid

(A) $^{13}C/^{12}C$ ratio images of bacterial cultures from a skin swab of a poison frog (left) or from fixed bacterial cultures (right) incubated in ^{13}C DHQ.

(B) Many individual regions of interest from the swab exhibited ^{13}C enrichment above the natural abundance of ^{13}C and the amount measured in killed controls, boxplots denote median with interquartile range (IQR) ± 1.5*IQR, dots are outlier points.

(C) To accomplish reverse labeling, bacterial strains were grown in ^{13}C-glucose to label the cells with ^{13}C and then were assayed for incorporation of natural abundance DHQ carbon based on subsequent dilution of ^{13}C.

(D) For both *Serratia* sp. and *Providencia* sp., $^{13}C/^{12}C$ ratios as measured with nanoSIMS decreased over a 48-h period.

(E) ^{13}C atom percent enrichment decreased significantly more across time in the DHQ treatment than in the control treatment, with no DHQ for both Serratia (upper) and *Providencia* (lower). ***$p < 0.001$, **$p < 0.01$, boxplots are IQR ± 1.5*IQR, dots are outlier points.

See also Figure S3.

Please cite this article in press as: Caty et al., Alkaloids are associated with increased microbial diversity and metabolic function in poison frogs, Current Biology (2024), https://doi.org/10.1016/j.cub.2024.10.069

(98.93% ^{12}C) (Figure 4C). We again used nanoSIMS to calculate the ^{13}C APE for samples taken at the beginning and end of the experiment (Figure 4D). We also included ^{15}N ammonium in the media as another metric of cell growth, determined by nitrogen incorporation. The results for *Serratia* are ambivalent because, although there was a greater decrease in ^{13}C enrichment in the DHQ treatment as compared with the methanol (carrier control) treatment (Figure 4E upper, $R^2 = 0.18$, $F_{3,\ 1,074} = 81.4$, treatment: time $p = 0.007$), the ^{13}C enrichment for the DHQ treatment at time 0 was higher than for the no-DHQ treatment. This could inflate the differences observed across groups, but we do not have an explanation for why the time 0 isotope enrichments were different for the two treatments. In addition, the ^{15}N enrichments from ammonium were similar (Figure S3A, $R^2 = 0.32$, $F_{3,\ 1,074} = 169.2$, treatment * time $p = 0.93$), suggesting no difference in growth. *Providencia* sp. incorporated more new carbon in the DHQ treatment compared with the no-DHQ treatment (Figure 4E lower, $R^2 = 0.36$, $F_{3,\ 2,860} = 535.2$, treatment:time $p < 0.001$). We observed that *Providencia* sp. uptake of ^{15}N-ammonium was below detection in both treatments. Based on the ^{13}C data (Figures 4E and S3B), *Providencia* sp. was growing, and, if it was maintaining stoichiometry, it may have used the nitrogen from DHQ for growth instead of from the labeled ammonium. These results suggest that *Providencia* sp. was able to utilize DHQ as a carbon source for growth—and potentially as a nitrogen source.

DISCUSSION

In this study, we found that alkaloids increased the diversity of poison frog skin microbial communities, particularly among rare taxa. A recent survey identified 27 common bacterial genera across many amphibian taxa.[24] Although 17 of these genera were found across all wild frogs in this study, there was zero overlap between the common genera and the genera found only on alkaloid-containing frogs, suggesting that the major taxa of poison frogs may be similar to that of non-poison frog species but that there are rare, specialist taxa whose presence may be modified by the presence of these alkaloids. Rare taxa can play outsized roles in microbial communities,[25] so these rare taxa may play a significant role in community function that is obscured by the minor changes in overall community structure.

Within the feeding experiment, where host species and environmental factors were removed, the presence of a single alkaloid did result in microbial community changes that differed across the tested frog species. In AF, a low-alkaloid species in the wild, the alkaloids did not change the microbial community composition, whereas the OS bacterial communities did shift, again seemingly through the addition of rare taxa. The fact that the AF communities were not dramatically impacted may be explained by recent work that has proposed alkaloid accumulation as an intermediate evolutionary step toward the chemically defended phenotype. This suggests that "non-toxic" dendrobatids, including AF, consume some alkaloids and accumulate them onto the skin.[26] This concept may not only explain the unexpected presence of DHQ that we observed on the skins of the DHQ-fed AF but may also explain why the microbial communities were not drastically impacted. It could be that infrequent, low levels of alkaloid exposure have created a selective environment where taxa that can tolerate this infrequent exposure persist. However, with the OS communities, not only might there be a selection for ability to survive but the high quantity and constant exposure may also create an environment for microbes with unique metabolic niches to survive, resulting in the observed shifts in structure and increase in these rare taxa. In other toxin-producing taxa, like boreal toads, which produce bufadienolides, or fire salamanders, which produce alkaloids, toxins also show evidence of shaping microbial communities.[27,28]

Together, the growth curves, metagenomic data, and nanoSIMS data provide some insights into potential mechanisms that the OS microbes may be using to deal with the alkaloids, including metabolism. Although alkaloid metabolism is relatively rare, it would be unsurprising for it to have arisen in the alkaloid-rich environment of poison frog skin. Similar microbial adaptations to toxic environments exist in other organisms, including herbivorous insects.[29–32] This phenomenon also occurs in the gut microbiota of the desert woodrat, which is able to metabolize the tannins and oxalates from the creosote plant, reducing the toxic effect on the host.[13,33,34] Similar to our results, exposure to a toxin that the woodrat host has experienced previously results in an increase in microbial community diversity, suggesting that this pattern may be generalizable across microbial communities in hosts that have evolved to consume high quantities of toxins. Although the metabolic pathways involved in the degradation of alkaloids are poorly characterized,[35] and therefore difficult to identify in metagenomic data, our metagenomic data do suggest a broader capacity for utilizing carbon and nitrogen in different ways, which may facilitate the utilization of alkaloid-derived carbon and nitrogen. Additionally, it is possible that another mechanism for survival in an alkaloid-rich environment is the increased capacity for microbes to remove the alkaloids from their cells. From the metagenomics data, OS communities had a greater number of transport-related genes than AF communities, which may facilitate the tolerance of high alkaloid loads, analogous to what has been observed in many microbial communities faced with environmental toxins.[36–39] This may also correspond to the tolerant phenotypes we observed in many isolates. Additional strategies that we were unable to explore in this work, including biofilm formation,[40–42] may also contribute to the community response to alkaloids. Further exploration of the mechanisms of alkaloid response may elucidate novel microbial functions.

We have demonstrated here that alkaloids play an important role in structuring the microbial communities of poison frogs, potentially mediated by the capability of isolates to metabolize alkaloids. This work broadens our understanding of how long-term exposure of a microbial community to exogenous compounds, in this case alkaloids, alters microbial community composition and provides additional avenues for exploration of microbial metabolism of alkaloids and the impact of alkaloid-induced microbiome shifts on host health.

RESOURCE AVAILABILITY

Lead contact

Requests for further information and resources should be directed to the lead contact, Lauren O'Connell (loconnel@stanford.edu).

Materials availability

Microbial isolates are available from the lead author upon request.

Data and code availability

- Field frog gas chromatography-mass spectrometry (GC-MS) data can be found on DataDryad: https://doi.org/10.5061/dryad.9ghx3ffqn and are publicly available as of the date of publication.
- Lab frog liquid chromatography-mass spectrometry (LC-MS) data can be found on DataDryad: https://doi.org/10.5061/dryad.gxd2547t1 and are publicly available as of the date of publication.
- Field frog 16S rRNA data can be found on DataDryad: https://doi.org/10.5061/dryad.5qfttdzd5 and are publicly available as of the date of publication.
- Field frog ITS data can be found on DataDryad: https://doi.org/10.5061/dryad.9cnp5hqrm and are publicly available as of the date of publication.
- Lab frog 16S rRNA data can be found on DataDryad: https://doi.org/10.5061/dryad.tdz08kq62 and are publicly available as of the date of publication.
- Lab frog ITS data can be found on DataDryad: https://doi.org/10.5061/dryad.4mw6m90hn and are publicly available as of the date of publication.
- Metagenomic data can be found on DataDryad: https://doi.org/10.5061/dryad.2ngf1vhzc and are publicly available as of the date of publication.
- All original code is available in this paper's supplemental information.
- Any additional information required to reanalyze the data reported in this paper is available from the lead contact upon request.

ACKNOWLEDGMENTS

We thank Courtney Swink and Christina Ramon for their assistance in conducting experiments at Lawrence Livermore National Laboratory. We thank the Relman lab at Stanford University for their input and suggestions on data analyses. We thank Tad Fukami for generously offering his lab space to perform the library preps and for guidance and suggestions about data analysis throughout. In Ecuador, Andrea Terán Valdez helped with permit procedures and coordinating field work. We thank Jeff Bishop at the University of Oregon Genomics and Cell Characterization Facility for completing the library preps and sequencing for the feeding experiment samples. The authors acknowledge that this research was conducted on the ancestral lands of the Muwekma Ohlone people at Stanford. We understand the implications of the historical and present colonialism the Ohlone people experience and celebrate their continued stewardship of their lands. This work was supported by the New York Stem Cell Foundation (L.A.O.). L.A.O. is a New York Stem Cell Foundation – Robertson investigator. S.N.C. is supported by an NSF Graduate Research Fellowship (DGE-1656518) and a Stanford Graduate Fellowship in Science and Engineering. A.A.-B. is supported by an NSF Graduate Research Fellowship (DGE-1656518) and an HHMI Gilliam Fellowship (www.hhmi.org, GT13330). Work at Lawrence Livermore National Laboratory was conducted under contract DE-AC52-07NA27344 and funded by microbiospheres Science Focus Area grant no. SCW1039 by the US Department of Energy's Office of Biological and Environmental Research. Part of this work was supported by the Vincent Coates Foundation Mass Spectrometry Laboratory, Stanford University Mass Spectrometry (RRID:SCR_017801), utilizing the Thermo Exploris 240 BioPharma LC/MS system (SCR_022216), and in part by NIH P30 CA124435, utilizing the Stanford Cancer Institute Proteomics/Mass Spectrometry Shared Resource. Figure 4B and portions of the graphical abstract were created in BioRender.

AUTHOR CONTRIBUTIONS

The study was conceptualized by S.N.C., M.M.M., X.M., and L.A.O. Data curation was performed by S.N.C. Formal analyses were conducted by S.N.C., M.M.M., T.M., and A.A.-B. Funding was acquired by L.A.O., X.M., P.K.W., and L.A.C. The investigation was performed by S.N.C., M.M.M., T.M., A.A.-B., N.A.M., C.V., E.E.T., and C.L.G. The methodology was developed by S.N.C., M.M.M., X.M., P.K.W., and T.M. Resources were provided by X.M. and L.A.O. The work was supervised by M.M.M., L.A.O., and L.A.C. Data visualization and initial draft writing was done by S.N.C. The manuscript was reviewed and edited by A.A.-B., X.M., P.K.W., C.V., N.A.M., T.M., L.A.O., E.E.T., L.A.C., and M.M.M.

DECLARATION OF INTERESTS

The authors declare no competing interests.

STAR★METHODS

Detailed methods are provided in the online version of this paper and include the following:

- KEY RESOURCES TABLE
- EXPERIMENTAL MODEL AND STUDY PARTICIPANT DETAILS
  - Field frogs
  - Laboratory Frogs
  - Bacterial and Fungal Strains
- METHOD DETAILS
  - Alkaloid extraction and quantification
  - DNA extraction from field swabs
  - Library preparation and sequencing of field swabs
  - Feeding experiment
  - Sequencing for feeding experiment samples
  - Feeding experiment alkaloid quantification
  - Metagenomics
  - Microbial isolate library characterization
  - Isotope labeling nanoSIMS experiments
- QUANTIFICATION AND STATISTICAL ANALYSIS
  - 16S rRNA and ITS amplicon sequencing analysis
  - Metagenomics analysis
  - Quantification of microbial growth with an alkaloid
  - NanoSIMS quantification

SUPPLEMENTAL INFORMATION

Supplemental information can be found online at https://doi.org/10.1016/j.cub.2024.10.069.

Received: January 11, 2024
Revised: September 15, 2024
Accepted: October 28, 2024
Published: December 4, 2024

REFERENCES

1. McFall-Ngai, M., Hadfield, M.G., Bosch, T.C.G., Carey, H.V., Domazet-Lošo, T., Douglas, A.E., Dubilier, N., Eberl, G., Fukami, T., Gilbert, S.F., et al. (2013). Animals in a bacterial world, a new imperative for the life sciences. Proc. Natl. Acad. Sci. USA *110*, 3229–3236. https://doi.org/10.1073/pnas.1218525110.
2. Sampson, T.R., and Mazmanian, S.K. (2015). Control of brain development, function, and behavior by the microbiome. Cell Host Microbe *17*, 565–576. https://doi.org/10.1016/j.chom.2015.04.011.
3. Dimmitt, R.A., Staley, E.M., Chuang, G., Tanner, S.M., Soltau, T.D., and Lorenz, R.G. (2010). Role of postnatal acquisition of the intestinal microbiome in the early development of immune function. J. Pediatr. Gastroenterol. Nutr. *51*, 262–273. https://doi.org/10.1097/MPG.0b013e3181e1a114.
4. Douglas, A.E. (1992). Requirement of pea aphids (Acyrthosiphon pisum) for their symbiotic bacteria. Entomol. Exp. Appl. *65*, 195–198. https://doi.org/10.1111/j.1570-7458.1992.tb01643.x.
5. Schmidt, T.S.B., Raes, J., and Bork, P. (2018). The human gut microbiome: from association to modulation. Cell *172*, 1198–1215. https://doi.org/10.1016/j.cell.2018.02.044.
6. Gould, A.L., Zhang, V., Lamberti, L., Jones, E.W., Obadia, B., Korasidis, N., Gavryushkin, A., Carlson, J.M., Beerenwinkel, N., and Ludington, W.B. (2018). Microbiome interactions shape host fitness. Proc. Natl. Acad. Sci. USA *115*, E11951–E11960. https://doi.org/10.1073/pnas.1809349115.

7. Antonopoulos, D.A., Huse, S.M., Morrison, H.G., Schmidt, T.M., Sogin, M.L., and Young, V.B. (2009). Reproducible Community Dynamics of the gastrointestinal microbiota following antibiotic Perturbation. Infect. Immun. *77*, 2367–2375. https://doi.org/10.1128/IAI.01520-08.

8. Langdon, A., Crook, N., and Dantas, G. (2016). The effects of antibiotics on the microbiome throughout development and alternative approaches for therapeutic modulation. Genome Med. *8*, 39. https://doi.org/10.1186/s13073-016-0294-z.

9. Tsiaoussis, J., Antoniou, M.N., Koliarakis, I., Mesnage, R., Vardavas, C.I., Izotov, B.N., Psaroulaki, A., and Tsatsakis, A. (2019). Effects of single and combined toxic exposures on the gut microbiome: current knowledge and future directions. Toxicol. Lett. *312*, 72–97. https://doi.org/10.1016/j.toxlet.2019.04.014.

10. Maurice, C.F., Haiser, H.J., and Turnbaugh, P.J. (2013). Xenobiotics shape the physiology and gene expression of the active human gut microbiome. Cell *152*, 39–50. https://doi.org/10.1016/j.cell.2012.10.052.

11. Carmody, R.N., Bisanz, J.E., Bowen, B.P., Maurice, C.F., Lyalina, S., Louie, K.B., Treen, D., Chadaideh, K.S., Maini Rekdal, V.M., Bess, E.N., et al. (2019). Cooking shapes the structure and function of the gut microbiome. Nat. Microbiol. *4*, 2052–2063. https://doi.org/10.1038/s41564-019-0569-4.

12. Shiffman, M.E., Soo, R.M., Dennis, P.G., Morrison, M., Tyson, G.W., and Hugenholtz, P. (2017). Gene and genome-centric analyses of koala and wombat fecal microbiomes point to metabolic specialization for Eucalyptus digestion. PeerJ *5*, e4075. https://doi.org/10.7717/peerj.4075.

13. Kohl, K.D., and Dearing, M.D. (2012). Experience matters: prior exposure to plant toxins enhances diversity of gut microbes in herbivores. Ecol. Lett. *15*, 1008–1015. https://doi.org/10.1111/j.1461-0248.2012.01822.x.

14. Saporito, R.A., Garraffo, H.M., Martin Garraffo, H.M., and Donnelly, M.A. (2009). Arthropod alkaloids in poison frogs: a review of the 'dietary hypothesis.' Heterocycles *79*, 277–297. https://doi.org/10.3987/REV-08-SR(D)11.

15. Saporito, R.A., Donnelly, M.A., Spande, T.F., and Garraffo, H.M. (2012). A review of chemical ecology in poison frogs. Chemoecology *22*, 159–168. https://doi.org/10.1007/s00049-011-0088-0.

16. Daly, J.W., Spande, T.F., and Garraffo, H.M. (2005). Alkaloids from amphibian skin: A tabulation of over eight-hundred compounds. J. Nat. Prod. *68*, 1556–1575. https://doi.org/10.1021/np0580560.

17. Daly, J.W. (1982). Biologically active alkaloids from poison frogs (Dendrobatidae). J. Toxicol. Toxin Rev. *1*, 33–86. https://doi.org/10.3109/15569548209016467.

18. Daly, J.W., Secunda, S.I., Garraffo, H.M., Spande, T.F., Wisnieski, A., Nishihira, C., and Cover, J.F. (1992). Variability in alkaloid profiles in Neotropical poison frogs (Dendrobatidae): genetic versus environmental determinants. Toxicon *30*, 887–898. https://doi.org/10.1016/0041-0101(92)90387-K.

19. Daly, J.W., Martin Garraffo, H., Spande, T.F., Jaramillo, C., and Stanley Rand, A. (1994). Dietary source for skin alkaloids of poison frogs (Dendrobatidae)? J. Chem. Ecol. *20*, 943–955. https://doi.org/10.1007/BF02059589.

20. Macfoy, C., Danosus, D., Sandit, R., Jones, T.H., Garraffo, H.M., Spande, T.F., and Daly, J.W. (2005). Alkaloids of anuran skin: antimicrobial function? Z. Naturforsch. C J. Biosci. *60*, 932–937. https://doi.org/10.1515/znc-2005-11-1218.

21. Mina, A.E., Ponti, A.K., Woodcraft, N.L., Johnson, E.E., and Saporito, R.A. (2015). Variation in alkaloid-based microbial defenses of the dendrobatid poison frog Oophaga pumilio. Chemoecology *25*, 169–178. https://doi.org/10.1007/s00049-015-0186-5.

22. Hovey, K.J., Seiter, E.M., Johnson, E.E., and Saporito, R.A. (2018). Sequestered alkaloid defenses in the dendrobatid poison frog Oophaga pumilio provide variable protection from microbial pathogens. J. Chem. Ecol. *44*, 312–325. https://doi.org/10.1007/s10886-018-0930-8.

23. Lin, H., and Peddada, S.D. (2020). Analysis of compositions of microbiomes with bias correction. Nat. Commun. *11*, 3514. https://doi.org/10.1038/s41467-020-17041-7.

24. Kueneman, J.G., Bletz, M.C., McKenzie, V.J., Becker, C.G., Joseph, M.B., Abarca, J.G., Archer, H., Arellano, A.L., Bataille, A., Becker, M., et al. (2019). Community richness of amphibian skin bacteria correlates with bioclimate at the global scale. Nat. Ecol. Evol. *3*, 381–389. https://doi.org/10.1038/s41559-019-0798-1.

25. Pascoal, F., Costa, R., and Magalhães, C. (2021). The microbial rare biosphere: current concepts, methods and ecological principles. FEMS Microbiol. Ecol. *97*, fiaa227. https://doi.org/10.1093/femsec/fiaa227.

26. Tarvin, R.D., Coleman, J.L., Donoso, D.A., Betancourth-Cundar, M., López-Hervas, K., Gleason, K.S., Sanders, J.R., Smith, J.M., Ron, S.R., Santos, J.C., et al. (2024). Passive accumulation of alkaloids in non-toxic frogs challenges paradigms of the origins of acquired chemical defenses. Preprint at bioRxiv. https://doi.org/10.1101/2024.05.13.593697.

27. Barnhart, K., Forman, M.E., Umile, T.P., Kueneman, J., McKenzie, V., Salinas, I., Minbiole, K.P.C., and Woodhams, D.C. (2017). Identification of bufadienolides from the Boreal Toad, Anaxyrus Boreas, Active against a Fungal Pathogen. Microb. Ecol. *74*, 990–1000. https://doi.org/10.1007/s00248-017-0997-8.

28. Sanchez, E., Bletz, M.C., Duntsch, L., Bhuju, S., Geffers, R., Jarek, M., Dohrmann, A.B., Tebbe, C.C., Steinfartz, S., and Vences, M. (2017). Cutaneous bacterial communities of a poisonous salamander: a perspective from life stages, body parts and environmental conditions. Microb. Ecol. *73*, 455–465. https://doi.org/10.1007/s00248-016-0863-0.

29. Shukla, S.P., and Beran, F. (2020). Gut microbiota degrades toxic isothiocyanates in a flea beetle pest. Mol. Ecol. *29*, 4692–4705. https://doi.org/10.1111/mec.15657.

30. Itoh, H., Tago, K., Hayatsu, M., and Kikuchi, Y. (2018). Detoxifying symbiosis: microbe-mediated detoxification of phytotoxins and pesticides in insects. Nat. Prod. Rep. *35*, 434–454. https://doi.org/10.1039/C7NP00051K.

31. van den Bosch, T.J.M., and Welte, C.U. (2017). Detoxifying symbionts in agriculturally important pest insects. Microb. Biotechnol. *10*, 531–540. https://doi.org/10.1111/1751-7915.12483.

32. Tang, Q., Li, W., Wang, Z., Dong, Z., Li, X., Li, J., Huang, Q., Cao, Z., Gong, W., Zhao, Y., et al. (2023). Gut microbiome helps honeybee (Apis mellifera) resist the stress of toxic nectar plant (Bidens pilosa) exposure: evidence for survival and immunity. Environ. Microbiol. *25*, 2020–2031. https://doi.org/10.1111/1462-2920.16436.

33. Kohl, K.D., Weiss, R.B., Cox, J., Dale, C., and Dearing, M.D. (2014). Gut microbes of mammalian herbivores facilitate intake of plant toxins. Ecol. Lett. *17*, 1238–1246. https://doi.org/10.1111/ele.12329.

34. Kohl, K.D., Connelly, J.W., Dearing, M.D., and Forbey, J.S. (2016). Microbial detoxification in the gut of a specialist avian herbivore, the Greater Sage-Grouse. FEMS Microbiol. Lett. *363*, fnw144. https://doi.org/10.1093/femsle/fnw144.

35. Rogowska-van der Molen, M.A., Berasategui-Lopez, A., Coolen, S., Jansen, R.S., and Welte, C.U. (2023). Microbial degradation of plant toxins. Environ. Microbiol. *25*, 2988–3010. https://doi.org/10.1111/1462-2920.16507.

36. Wang, S., Gao, X., Gao, Y., Li, Y., Cao, M., Xi, Z., Zhao, L., and Feng, Z. (2017). Tetracycline resistance genes identified from distinct soil environments in china by functional metagenomics. Front. Microbiol. *8*, 1406. https://doi.org/10.3389/fmicb.2017.01406.

37. Diba, F., Hoque, M.N., Rahman, M.S., Haque, F., Rahman, K.M.d.J., Moniruzzaman, M.d., Khan, M., Hossain, M.A., and Sultana, M. (2023). Metagenomic and culture-dependent approaches unveil active microbial community and novel functional genes involved in arsenic mobilization and detoxification in groundwater. BMC Microbiol. *23*, 241. https://doi.org/10.1186/s12866-023-02980-0.

38. Li, J., Jia, C., Lu, Q., Hungate, B.A., Dijkstra, P., Wang, S., Wu, C., Chen, S., Li, D., and Shim, H. (2021). Mechanistic insights into the success of xenobiotic degraders resolved from metagenomes of microbial enrichment cultures. J. Hazard. Mater. *418*, 126384. https://doi.org/10.1016/j.jhazmat.2021.126384.

39. Mittal, P., Prasoodanan Pk, V., Dhakan, D.B., Kumar, S., and Sharma, V.K. (2019). Metagenome of a polluted river reveals a reservoir of metabolic and

antibiotic resistance genes. Environ. Microbiome *14*, 5. https://doi.org/10.1186/s40793-019-0345-3.

40. Chen, M.Y., Alexiev, A., and McKenzie, V.J. (2022). Bacterial biofilm thickness and fungal inhibitory bacterial richness both prevent establishment of the amphibian fungal pathogen Batrachochytrium dendrobatidis. Appl. Environ. Microbiol. *88*, e0160421. https://doi.org/10.1128/aem.01604-21.
41. Wicaksono, W.A., Erschen, S., Krause, R., Müller, H., Cernava, T., and Berg, G. (2022). Enhanced survival of multi-species biofilms under stress is promoted by low-abundant but antimicrobial-resistant keystone species. J. Hazard. Mater. *422*, 126836. https://doi.org/10.1016/j.jhazmat.2021.126836.
42. Dusane, D.H., Hosseinidoust, Z., Asadishad, B., and Tufenkji, N. (2014). Alkaloids modulate motility, biofilm formation and antibiotic susceptibility of uropathogenic Escherichia coli. PLoS One *9*, e112093. https://doi.org/10.1371/journal.pone.0112093.
43. Walters, W., Hyde, E.R., Berg-Lyons, D., Ackermann, G., Humphrey, G., Parada, A., Gilbert, J.A., Jansson, J.K., Caporaso, J.G., Fuhrman, J.A., et al. (2016). Improved bacterial 16S rRNA gene (V4 and V4-5) and Fungal Internal Transcribed Spacer Marker Gene Primers for Microbial Community Surveys. mSystems *1*, e00009–e00015. https://doi.org/10.1128/mSystems.00009-15.
44. Fredriksson, N.J., Hermansson, M., and Wilén, B.-M. (2013). The choice of PCR primers has great impact on assessments of bacterial community diversity and dynamics in a wastewater treatment plant. PLoS One *8*, e76431. https://doi.org/10.1371/journal.pone.0076431.
45. White, T.J., Bruns, T., Lee, S., and Taylor, J. (1990). Amplification and direct sequencing of fungal ribosomal RNA genes for phylogenetics. In PCR Protocols, *38*, M.A. Innis, D.H. Gelfand, J.J. Sninsky, and T.J. White, eds. (Academic Press), pp. 315–322. https://doi.org/10.1016/B978-0-12-372180-8.50042-1.
46. Ihrmark, K., Bödeker, I.T.M., Cruz-Martinez, K., Friberg, H., Kubartova, A., Schenck, J., Strid, Y., Stenlid, J., Brandström-Durling, M., Clemmensen, K.E., et al. (2012). New primers to amplify the fungal ITS2 region–evaluation by 454-sequencing of artificial and natural communities. FEMS Microbiol. Ecol. *82*, 666–677. https://doi.org/10.1111/j.1574-6941.2012.01437.x.
47. López-Hervas, K., Santos, J.C., Ron, S.R., Betancourth-Cundar, M., Cannatella, D.C., and Tarvin, R.D. (2024). Deep divergences among inconspicuously colored clades of *Epipedobates* poison frogs. Mol. Phylogenet. Evol. *195*, 108065. https://doi.org/10.1016/j.ympev.2024.108065.
48. Caty, S.N., Vasek, C., Fischer, M.-T., Meneses, A.M., Shaykevich, D.A., and O'Connell, L.A. (2024). Isolation of microbes from the skin of terrestrial frogs. Preprint at bioRxiv. https://doi.org/10.1101/2024.09.11.612488.
49. Alvarez-Buylla, A., Fischer, M.-T., Moya Garzon, M.D., Rangel, A.E., Tapia, E.E., Tanzo, J.T., Soh, H.T., Coloma, L.A., Long, J.Z., and O'Connell, L.A. (2023). Binding and sequestration of poison frog alkaloids by a plasma globulin. eLife *12*, e85096. https://doi.org/10.7554/eLife.85096.
50. Saporito, R.A., Isola, M., Maccachero, V.C., Condon, K., and Donnelly, M.A. (2010). Ontogenetic scaling of poison glands in a dendrobatid poison frog. J. Zool. *282*, 238–245. https://doi.org/10.1111/j.1469-7998.2010.00732.x.
51. Wang, M., Carver, J.J., Phelan, V.V., Sanchez, L.M., Garg, N., Peng, Y., Nguyen, D.D., Watrous, J., Kapono, C.A., Luzzatto-Knaan, T., et al. (2016). Sharing and community curation of mass spectrometry data with Global Natural Products Social Molecular Networking. Nat. Biotechnol. *34*, 828–837. https://doi.org/10.1038/nbt.3597.
52. Hamady, M., Walker, J.J., Harris, J.K., Gold, N.J., and Knight, R. (2008). Error-correcting barcoded primers allow hundreds of samples to be pyrosequenced in multiplex. Nat. Methods *5*, 235–237. https://doi.org/10.1038/nmeth.1184.
53. Sanchez, E., Rodríguez, A., Grau, J.H., Lötters, S., Künzel, S., Saporito, R.A., Ringler, E., Schulz, S., Wollenberg Valero, K.C., and Vences, M. (2019). Transcriptomic signatures of experimental alkaloid consumption in a poison frog. Genes *10*, 733. https://doi.org/10.3390/genes10100733.
54. Minich, J.J., Humphrey, G., Benitez, R.A.S., Sanders, J., Swafford, A., Allen, E.E., and Knight, R. (2018). High-throughput miniaturized 16S rRNA amplicon library preparation reduces costs while preserving microbiome integrity. mSystems *3*, e00166-18. https://doi.org/10.1128/msystems.00166-18.
55. Samo, T.J., Kimbrel, J.A., Nilson, D.J., Pett-Ridge, J., Weber, P.K., and Mayali, X. (2018). Attachment between heterotrophic bacteria and microalgae influences symbiotic microscale interactions. Environ. Microbiol. *20*, 4385–4400. https://doi.org/10.1111/1462-2920.14357.
56. Pett-Ridge, J., and Weber, P.K. (2012). NanoSIP: NanoSIMS applications for microbial biology. Methods Mol. Biol. Clifton NJ *881*, 375–408. https://doi.org/10.1007/978-1-61779-827-6_13.
57. Callahan, B.J., McMurdie, P.J., Rosen, M.J., Han, A.W., Johnson, A.J.A., and Holmes, S.P. (2016). DADA2: high-resolution sample inference from Illumina amplicon data. Nat. Methods *13*, 581–583. https://doi.org/10.1038/nmeth.3869.
58. Martin, M. (2011). Cutadapt removes adapter sequences from high-throughput sequencing reads. EMBnet.journal *17*, 10–12. https://doi.org/10.14806/ej.17.1.200.
59. Schliep, K.P. (2011). phangorn: phylogenetic analysis in R. Bioinformatics *27*, 592–593. https://doi.org/10.1093/bioinformatics/btq706.
60. McMurdie, P.J., and Holmes, S. (2013). phyloseq: an R package for Reproducible Interactive Analysis and Graphics of microbiome Census Data. PLoS One *8*, e61217. https://doi.org/10.1371/journal.pone.0061217.
61. Kembel, S.W., Cowan, P.D., Helmus, M.R., Cornwell, W.K., Morlon, H., Ackerly, D.D., Blomberg, S.P., and Webb, C.O. (2010). Picante: R tools for integrating phylogenies and ecology. Bioinformatics *26*, 1463–1464. https://doi.org/10.1093/bioinformatics/btq166.
62. Simmons, M.P., and Freudenstein, J.V. (2003). The effects of increasing genetic distance on alignment of, and tree construction from, rDNA internal transcribed spacer sequences. Mol. Phylogenet. Evol. *26*, 444–451. https://doi.org/10.1016/S1055-7903(02)00366-4.
63. Oksanen, J., Simpson, G., Blanchet, F., Kindt, R., Legendre, P., Minchin, P., O'Hara, R., Solymos, P., Stevens, M., Szoecs, E., et al. (2024). vegan: community Ecology Package. R package. version 2.6-6.1. https://CRAN.R-project.org/package=vegan.
64. Grant, T., Rada, M., Anganoy-Criollo, M., Batista, A., Dias, P.H., Jeckel, A.M., Machado, D.J., and Rueda-Almonacid, J.V. (2017). Phylogenetic systematics of dart-poison frogs and their relatives revisited (Anura: Dendrobatoidea). S. Am. J. Herpetol. *12*, S1–S90. https://doi.org/10.2994/SAJH-D-17-00017.1.
65. Paradis, E., Claude, J., and Strimmer, K. (2004). APE: analyses of Phylogenetics and Evolution in R language. Bioinformatics *20*, 289–290. https://doi.org/10.1093/bioinformatics/btg412.
66. Bolker, B., Butler, M., Cowan, P., de Vienne, D., Eddelbuettel, D., Holder, M., Jombart, T., Kembel, S., Michonneau, F., Orme, D., et al.. phylobase: Base Package for Phylogenetic Structures and Comparative Data. v0.8.12 CRAN. https://rdrr.io/cran/phylobase/.
67. Hijmans, R. (2022). geosphere: Spherical Trigonometry. R package version 1.5-18. https://CRAN.R-project.org/package=geosphere.
68. Goslee, S.C., and Urban, D.L. (2007). The ecodist Package for Dissimilarity-based Analysis of Ecological Data. J. Stat. Softw. *22*, 1–19. https://doi.org/10.18637/jss.v022.i07.
69. Weinstein, S.B., Martínez-Mota, R., Stapleton, T.E., Klure, D.M., Greenhalgh, R., Orr, T.J., Dale, C., Kohl, K.D., and Dearing, M.D. (2021). Microbiome stability and structure is governed by host phylogeny over diet and geography in woodrats (Neotoma spp.). Proc. Natl. Acad. Sci. USA *118*, e2108787118. https://doi.org/10.1073/pnas.2108787118.
70. Galili, T. (2015). dendextend: an R package for visualizing, adjusting and comparing trees of hierarchical clustering. Bioinformatics *31*, 3718–3720. https://doi.org/10.1093/bioinformatics/btv428.
71. Huang, R., Soneson, C., Ernst, F.G.M., Rue-Albrecht, K.C., Yu, G., Hicks, S.C., and Robinson, M.D. (2020). TreeSummarizedExperiment: a S4 class

for data with hierarchical structure. F1000Res *9*, 1246. https://doi.org/10.12688/f1000research.26669.2.

72. Ernst, F., Shetty, S., Borman, T., and Lahti, L. (2024). mia: Microbiome analysis. R package version 1.12.0. https://doi.org/10.18129/B9.bioc.mia.
73. Xie, Y., Cheng, J., Tan, X., Allaire, J.J., Girlich, M., Ellis, G.F., and Rauh, J. (2024). DT: A Wrapper of the JavaScript Library "DataTables". Version 0.33. https://cran.r-project.org/web/packages/DT/index.html.
74. Roberts, D.W. (2023). labdsv: Ordination and Multivariate Analysis for Ecology. Version 2.1-0.
75. Warnes, G.R., Bolker, B., Bonebakker, L., Gentleman, R., Huber, W., Liaw, A., Lumley, T., Maechler, M., Magnusson, A., Moeller, S., et al. (2024). gplots: Various R Programming Tools for Plotting Data. Version 3.1.3.1.
76. Wickham, H., Vaughan, D., and Girlich, M. (2024). tidyr: Tidy Messy Data. R package version 1.3.1. https://CRAN.R-project.org/package=tidyr.
77. Wickham, H., François, R., Henry, L., Müller, K., and Vaughan, D. (2023). dplyr: A Grammar of Data Manipulation. R package version 1.1.4. https://CRAN.R-project.org/package=dplyr.
78. Wickham, H. (2016). ggplot2: Elegant Graphics for Data Analysis (Springer-Verlag New York).
79. Arkin, A.P., Cottingham, R.W., Henry, C.S., Harris, N.L., Stevens, R.L., Maslov, S., Dehal, P., Ware, D., Perez, F., Canon, S., et al. (2018). KBase: the United States Department of Energy systems biology knowledgebase. Nat. Biotechnol. *36*, 566–569. https://doi.org/10.1038/nbt.4163.
80. Bolger, A.M., Lohse, M., and Usadel, B. (2014). Trimmomatic: a flexible trimmer for Illumina sequence data. Bioinformatics *30*, 2114–2120. https://doi.org/10.1093/bioinformatics/btu170.
81. Babraham Bioinformatics. FastQC A Quality Control tool for High Throughput Sequence Data. https://www.bioinformatics.babraham.ac.uk/projects/fastqc/.
82. Nurk, S., Meleshko, D., Korobeynikov, A., and Pevzner, P.A. (2017). metaSPAdes: a new versatile metagenomic assembler. Genome Res. *27*, 824–834. https://doi.org/10.1101/gr.213959.116.
83. Shaffer, M., Borton, M.A., McGivern, B.B., Zayed, A.A., La Rosa, S.L., Solden, L.M., Liu, P., Narrowe, A.B., Rodríguez-Ramos, J., Bolduc, B., et al. (2020). DRAM for distilling microbial metabolism to automate the curation of microbiome function. Nucleic Acids Res. *48*, 8883–8900. https://doi.org/10.1093/nar/gkaa621.
84. Hughes, S. (2022). plater: Read, Tidy, and Display Data from Microtiter Plates. Version 1.0.4.
85. Sprouffske, K., and Wagner, A. (2016). Growthcurver: an R package for obtaining interpretable metrics from microbial growth curves. BMC Bioinformatics *17*, 172. https://doi.org/10.1186/s12859-016-1016-7.
86. Popa, R., Weber, P.K., Pett-Ridge, J., Finzi, J.A., Fallon, S.J., Hutcheon, I.D., Nealson, K.H., and Capone, D.G. (2007). Carbon and nitrogen fixation and metabolite exchange in and between individual cells of Anabaena oscillarioides. ISME J. *1*, 354–360. https://doi.org/10.1038/ismej.2007.44.

Please cite this article in press as: Caty et al., Alkaloids are associated with increased microbial diversity and metabolic function in poison frogs, Current Biology (2024), https://doi.org/10.1016/j.cub.2024.10.069

STAR★METHODS

KEY RESOURCES TABLE

REAGENT or RESOURCE	SOURCE	IDENTIFIER
Bacterial and virus strains		
Brachybacterium rhamnosum	This paper	N/A
Pseudomonas alcaligenes	This paper	N/A
Stenotrophomonas rhizophila	This paper	N/A
Domibacillus endensis	This paper	N/A
Brevibacterium sediminis	This paper	N/A
Citrobacter braakii	This paper	N/A
Domibacillus robiginosus	This paper	N/A
Variovorax soli	This paper	N/A
Pseudoclavibacter bifida	This paper	N/A
Rhodococcus pedocola	This paper	N/A
Glutamicibacter protophormiae	This paper	N/A
Acinetobacter johnsonii	This paper	N/A
Beijerinckia fluminensis	This paper	N/A
Microbacterium aureliae	This paper	N/A
Flavobacterium cerinum	This paper	N/A
Comamonas testosteroni	This paper	N/A
Pseudomonas mosselii	This paper	N/A
Plectosphaerellaceae sp.	This paper	N/A
Pseudomonas entomophila	This paper	N/A
Chryseobacterium indologenes	This paper	N/A
Providencia rettgeri	This paper	N/A
Serratia nematodiphila	This paper	N/A
Delftia acidovorans	This paper	N/A
Sphingobacterium multivorum	This paper	N/A
Chryseobacterium indoltheticum	This paper	N/A
Pseudomonas plecoglossicida	This paper	N/A
Aeromonas caviae	This paper	N/A
Acinetobacter bereziniae	This paper	N/A
Stenotrophomonas maltophilia	This paper	N/A
Acinetobacter modestus	This paper	N/A
Pseudomonas monteilii	This paper	N/A
Staphylococcus succinus	This paper	N/A
Serratia surfactantfaciens	This paper	N/A
Variovorax guangxiensis	This paper	N/A
Chryseobacterium culicis	This paper	N/A
Citrobacter freundii	This paper	N/A
Corynebacterium terpenotabidum	This paper	N/A
Pseudomonas koreensis	This paper	N/A
Microbacterium indicum	This paper	N/A
Rhodococcus cercidiphylli	This paper	N/A
Exiguobacterium indicum	This paper	N/A
Acinetobacter venetianus	This paper	N/A
Bacillus thuringiensis	This paper	N/A

(*Continued on next page*)

Please cite this article in press as: Caty et al., Alkaloids are associated with increased microbial diversity and metabolic function in poison frogs, Current Biology (2024), https://doi.org/10.1016/j.cub.2024.10.069

Continued

REAGENT or RESOURCE	SOURCE	IDENTIFIER
Staphylococcus sciuri	This paper	N/A
Staphylococcus xylosus	This paper	N/A
Biological samples		
Allobates femoralis (wild)	This paper	N/A
Allobates talamancae	This paper	N/A
Allobates zaparo	This paper	N/A
Ameerega bilinguis	This paper	N/A
Ameerega parvula	This paper	N/A
Epipedobates boulengeri	This paper	N/A
Epipedobates darwinwallacei	This paper	N/A
Epipedobates tricolor	This paper	N/A
Hyloxalus infraguttatus	This paper	N/A
Hyloxalus toachi	This paper	N/A
Oophaga sylvatica (wild)	This paper	N/A
Allobates femoralis (lab experiment)	Indoor Ecosystems	Allobates femoralis
Oophaga sylvatica (lab experiment)	Indoor Ecosystems	Oophaga sylvatica Paru
Chemicals, peptides, and recombinant proteins		
Decahydroquinoline, mixture of cis and trans	Santa Cruz Biotechnology	Cat#: sc-227742; CAS 2051-28-7
(-)-nicotine	Sigma Aldrich	Cat#: N3876-5ML; CAS 54-11-5
^{13}C DHQ	Cambridge Isotope Laboratories	Custom order
^{13}C glucose (99% ^{13}C)	Cambridge Isotope Laboratories	Cat#: CLM-1396-25
$^{15}NH_4Cl$ (99% ^{15}N)	Cambridge Isotope Laboratories	Cat#: NLM-467-PK
Critical commercial assays		
DNeasy PowerSoil Pro Kit	Qiagen	Cat#: 47016
FlashGel™ system & DNA Ladder	Lonza	Cat#: 57067 & 50473
NexteraXT library prep kit	Illumina	Cat#: FC-131-1096
E.Z.N.A Cycle Pure Kit	Omega Bio-Tek	Cat#: D6492-00
DNeasy Blood and Tissue Kit	Qiagen	Cat#: 69504
Deposited data		
Wild poison frog 16S Data	This paper	DataDryad: https://doi.org/10.5061/dryad.5qfttdzd5
Wild poison frog ITS Data	This paper	DataDryad: https://doi.org/10.5061/dryad.9cnp5hqrm
O. sylvatica and *A. femoralis* lab 16S data	This paper	DataDryad: https://doi.org/10.5061/dryad.tdz08kq62
O. sylvatica and *A. femoralis* lab ITS data	This paper	DataDryad: https://doi.org/10.5061/dryad.4mw6m90hn
Metagenomics data	This paper	DataDryad: https://doi.org/10.5061/dryad.2ngf1vhzc
Alkaloid field data	This paper	DataDryad: https://doi.org/10.5061/dryad.9ghx3ffqn
Feeding experiment alkaloid quantification	This paper	DataDryad: https://doi.org/10.5061/dryad.gxd2547t1
Oligonucleotides		
nexF-N_{3-6}-515f 5'-GTGYCAGCMG CCGCGGTAA-3'	Walters et al.[43]	N/A
nexF-N_{3-6}-806r 5'-GGACTACNV GGGTWTCTAAT-3'	Walters et al.[43]	N/A
nexF-N_{3-6}-ITS1f-KYO1 5' CTHGG TCATTTAGAGGAASTAA-3'	Walters et al.[43]	N/A

(*Continued on next page*)

Please cite this article in press as: Caty et al., Alkaloids are associated with increased microbial diversity and metabolic function in poison frogs, Current Biology (2024), https://doi.org/10.1016/j.cub.2024.10.069

Continued

REAGENT or RESOURCE	SOURCE	IDENTIFIER
nexF-N_{3-6}-ITS2-KYO2 5'-TTYR CTRCGTTCTTCATC-3'	Walters et al.[43]	N/A
27F (5'-AGAGTTTGATCMTGGCTCAG-3')	Fredriksson et al.[44]	N/A
1492R (5'-TACGGYTACCTTGTTAYGACTT-3')	Fredriksson et al.[44]	N/A
ITS4 (5'-TCCTCCGCTTATTGATATGC-3')	White et al.[45]	N/A
gITS7 (5'-GTGARTATCGARTCTTTG-3)	Ihrmark et al.[46]	N/A
Software and algorithms		
GNPS	UCSD	RRID:SCR_019012; https://gnps.ucsd.edu/
NIST Standard Reference Data	NIST	RRID:SCR_006452; http://www.nist.gov/srd/
Geneious Prime	Geneious	RRID:SCR_010519; https://www.geneious.com/
R	CRAN	RRID:SCR_001905; http://www.r-project.org/
Python	Python	RRID:SCR_008394; http://www.python.org/
Silva NR99 version 138.1	Leibniz Institute	RRID:SCR_006423; http://www.arb-silva.de
UNITE version 29.11.2022	University of Tartu	RRID:SCR_006518; http://unite.ut.ee/index.php
KBase	US Department of Energy	RRID:SCR_022162; https://www.kbase.us/
L'image	Larry Nittler, Arizona Staate University	https://sites.google.com/carnegiescience.edu/limagesoftware/
IDL virtual machine	NV5 Geospatial Software;	https://www.nv5geospatialsoftware.com/Support/Maintenance-Detail/the-idl-virtual-machine
Cameca nanoSIMS software	V 4.5	https://www.cameca.com/products/sims/nanosims

EXPERIMENTAL MODEL AND STUDY PARTICIPANT DETAILS

Field frogs

Individuals from 11 species of dendrobatid frogs (*Ameerega bilinguis*, *Ameerega parvula*, *Oophaga sylvatica*, *Epipedobates tricolor*, *Epipedobates boulengeri*, *Epipedobates darwinwallacei*, *Hyloxalus toachi*, *Hyloxalus infraguttatus*, *Allobates zaparo*, *Allobates talamancae*, and *Allobates femoralis*) were collected from 9 locations throughout Ecuador (Figure 1A; Table S1). Since collection, a new categorization of the Epipedobates genus has been published which may impact some of the species delineations of our samples, however we do not believe this will impact the overall findings of the paper.[47] An effort was made to collect roughly equal numbers of male and female frogs, however sex was not considered as a variable of analysis due to the limited sample size and a desire to not collect more frogs than was necessary. Animals were caught during the day and stored individually in moist plastic bags until the evening when frogs were rinsed with sterile water and swabbed 10 times (up and back is once) with sterile cotton swabs (Puritan 25-806 2WC). After swabbing, frogs were anesthetized with topical application of benzocaine and euthanized by cervical transection. Swabs were immediately placed into 100% ethanol and kept at -20 °C for long-term storage. Half of the dorsal skin from each frog was stored in methanol for alkaloid analyses until shipment to the US, wherein they were stored at -20 °C. Collections and exportation of specimens were done under permits (No. 0013-18 IC-FAU-DNB/MA; Export permit: No. 214-2019-EXP-CM-FAU-DNB/MA; CITES export permit No. 19EC000036/VS) issued by the Ministerio de Ambiente de Ecuador. All procedures were approved by the Administrative Panel on Laboratory Animal Care Committee of Stanford University (Protocol 34153).

Laboratory Frogs

Lab-raised Diablito frogs (*Oophaga sylvatica*, N=12) and brilliant thighed frogs (*Allobates femoralis*, N=12) were purchased from Indoor Ecosystems (Whitehouse, OH, USA). During the experiment, frogs were housed individually in plastic containers (Sterilite 16428012) with moist, autoclaved paper towels and plastic reptile hides (XYZ Reptiles, Palmetto Bay, FL, USA). Paper towels were replaced daily and sprayed with new sterile water to maintain humidity in the boxes. Frogs were fed $\sim$ $^1/_8$ teaspoon of fruit flies dusted with calcium powder (Repashy Calcium Plus) and vitamin powder (RepCal Herptivite) daily during the experiment. All procedures were approved by Administrative Panel on Laboratory Animal Care Committee of Stanford University (protocol #33691).

Please cite this article in press as: Caty et al., Alkaloids are associated with increased microbial diversity and metabolic function in poison frogs, Current Biology (2024), https://doi.org/10.1016/j.cub.2024.10.069

Bacterial and Fungal Strains

Microbial isolate libraries were made from swabs from laboratory reared, non-toxic *Oophaga sylvatica* that had not been used in the feeding experiments.[48] Swabs were immediately struck out onto solid media plates. Multiple media types were used to encourage higher diversity of cultivated isolates. The five media types used included 1% tryptone media (tryptone: Fisher BioReagents, Fisher Scientific), R2A (BD Difco, Fisher Scientific), LB (BD Difco, Fisher Scientific), tryptic soy agar with sheep's blood (pre-made plates: Thermo Scientific; tryptic soy agar: BD Difco, Fisher Scientific; defibrinated sheep's blood: Thermo Scientific, Fisher Scientific), and M9 minimal media (BD Difco, Fisher Scientific) with 0.01% w/v decahydroquinoline (Santa Cruz Biotechnology) as the sole carbon source. Plates were sealed with Parafilm and incubated at 21 °C.

METHOD DETAILS

Alkaloid extraction and quantification

Skins were processed for alkaloid extractions as described in Alvarez-Buylla et al. (2023).[49] Briefly, the methanol in which the skin was stored was filtered and spiked with (-)-nicotine (Sigma Aldrich, N3876-100ML), then stored at -80 °C for 24 hours to precipitate lipids and proteins. After filtering into new vials, a 100 μL aliquot was added to a gas chromatography / mass spectrometry (GC/MS) autosampler vial. GC/MS analysis was performed on a Shimadzu GCMS-QP2020 instrument with a Shimadzu 30 m x 0.25 mmID SH-Rxi-5Sil MS column closely following the protocol outlined in Saporito et al. (2010).[50] In brief, separation of alkaloids was achieved with helium as the carrier gas (flow rate: 1 mL/min) using a temperature program from 100 to 280 °C at a rate of 10 °C/min. This was followed by a 2 min hold and additional ramp to 320 °C at a rate of 10 °C/min for column protection reasons, and no alkaloids appeared during this part of the method. Compounds were analyzed with electron impact-mass spectrometry (EI-MS). The GC-MS data files were exported as CDF files and the Global Natural Products Social Molecular Networking (GNPS) software was used to perform the deconvolution and library searching against the AMDIS (NIST) database to identify all compounds.[51] For deconvolution (identification of peaks and abundance estimates) the default parameters were used. Through the deconvolution process, molecular features were reported as rows/observations, while m/z intensities were reported as columns/variables. Automatic library search was obtained from reference libraries of natural products (NIST, Wiley, University of CORSICA, GNPS), and our resulting dataset was filtered to keep only our nicotine standard and alkaloids previously found in poison frogs from the Daly et al. (2005) database, or compounds with the same base ring structure and R group positions as the classes defined in Daly et al. (2005).[16] Once the feature table from the GNPS deconvolution was filtered to include only poison frog alkaloids and nicotine, the abundance values (ion counts) were normalized by dividing by the nicotine standard and skin weight, and we included the 10 top database hits in our library search. The resulting filtered and normalized feature table was used for all further analyses and visualizations. All normalization steps were carried out with R (version 4.0.4).

DNA extraction from field swabs

Swabs in ethanol were stored at -20°C until DNA extraction. DNA was extracted from swabs using the Qiagen PowerSoil Pro Kit, adapted for use with swabs stored in ethanol. Briefly, swabs were quickly (2-3 s) vortexed in ethanol and dried at 37 °C (approximately 2 hours). The remaining ethanol was centrifuged at 15294 rcf for 15 min. The ethanol was discarded, and the pellet was washed once with 200 μL PBS, then centrifuged at 15294 rcf for 5 min. After removal of PBS, 800 μL of lysis buffer (CD1) was added to the pellet and allowed to incubate at room temperature for 10 min, after which the solution was transferred, along with the dried swab, to the PowerBead Pro Tube. Swabs were included through the addition of solution CD2, at which point swabs were removed and the protocol continued per manufacturer instructions. Solution C6 was allowed to incubate for 10 min prior to centrifugation. Extracted DNA was stored at -20 °C for prolonged storage, and 4 °C when in use. A DNA extraction control was generated by completing the entire process on a sterile swab.

Library preparation and sequencing of field swabs

Frog skin microbial community composition was described through amplification and sequencing of the taxonomy-inferring 16S rRNA gene for bacteria (V4 region) and internally transcribed spacer (ITS) gene for fungi (ITS1-2 region). Samples were randomly distributed across 96 well plates, with one well on each plate reserved as a PCR1 no DNA control and another well reserved as a PCR2 no DNA control to identify contaminants. In each well, 4.2 μL of extracted DNA was combined with 5 μL of MyTaq Red polymerase (Bioline, Meridian Bioscience), 0.4 μL of 10 μM forward primer (nexF-$N_{3\text{-}6}$-515f 5'-GTGYCAGCMGCCGCGGTAA-3' for 16S rRNA or nexF-$N_{3\text{-}6}$-ITS1f-KYO1 5'-CTHGGTCATTTAGAGGAASTAA-3' for ITS), and 0.4 μL of 10 μM reverse primer (nexF-$N_{3\text{-}6}$-806r 5'-GGACTACNVGGGTWTCTAAT-3' for 16S rRNA or nexF-$N_{3\text{-}6}$-ITS2-KYO2 5'-TTYRCTRCGTTCTTCATC-3' for ITS).[43] 16S rRNA PCR parameters were as follows: denaturation at 95 °C for 2 min followed by 35 cycles of denaturation at 95 °C for 20 s, annealing at 52.5 °C for 20 s, and extension at 72 °C for 50 s with a final extension of 10 min at 72 °C. The same protocol was used for ITS amplification with 50 °C used as the annealing temperature. Amplification of PCR 1 product and lack of amplification of PCR1 no DNA controls was confirmed from 12 randomly selected samples per 96 well plate using the Lonza FlashGel™ system (Lonza, 57067) with the FlashGel™ DNA Marker Ladder (Lonza, 50473) for size confirmation. Samples were subsequently barcoded in the second PCR using unique combinations of P5-Hamady-nexF and P7-Hamady-nexR primers.[52] For this PCR, 1 μL of template DNA from PCR 1 was added to 5 μL of MyTaq Red, 3.2 μL of water, and 0.8 μL of 10 μM primer (combination of forward and reverse). Samples were amplified with the following protocol: denaturation at 95 °C for 2 min followed by 8 cycles of denaturation at 95 °C for

20 s, annealing at 50 °C for 20 s, and extension at 72 °C for 50 s, followed by a final extension of 10 min at 72 °C. PCR products were cleaned and size selected with AMPure Beads in a ratio of sample to beads of 1:1.2. All 16S libraries were pooled in equal volumes and all ITS libraries were separately pooled in equal volumes. Pooled libraries were run on an Agilent TapeStation to confirm adequate size distribution (a peak around 450 bp) and quantified with a Qubit Fluorometer (Thermo Fisher Scientific). Samples were sequenced by Azenta Life Sciences (Burlington, MA, USA) with a 2x250 Illumina MiSeq configuration with an estimated coverage of ~50,000 reads per sample, with a 20% PhiX spike-in.

Feeding experiment

Within each species, frogs were split into two groups: those fed the alkaloid decahydroquinoline (DHQ, Santa Cruz Biotechnology, Santa Cruz CA, USA, N=6) and those fed a water vehicle control (N=6). Frogs from the same group housing tanks were split between two treatment groups, and sex was roughly evenly distributed across the two groups. Frogs were allowed to acclimate to their new housing for one week, after which (Day 8 and on) they were swabbed daily for the remainder of the experiment using Puritan Sterile Tipped Polyester Applicators (Puritan Medical Products, 25-206 1PD BT). Alkaloid feeding began 5 days after the onset of swabbing (Day 13) and continued for the duration of the experiment, for a total of 10 days. Prior alkaloid feeding experiments have been conducted with *A. femoralis*,[53] however, we observed signs of illness in two of the *A. femoralis* in the toxin feeding group on Day 19, and the experiment was immediately terminated for all *A. femoralis* at this point. Frogs fed decahydroquinoline (DHQ) were fed 10 μL of a 0.01% DHQ in water solution daily via pipetting directly into the mouth. Control frogs were fed 10 μL of water in the same manner daily. Swabbing occurred prior to alkaloid feeding on days when both occurred. Swabs were immediately placed on ice after collection and subsequently stored at -20 °C until DNA extraction. All procedures were approved by Administrative Panel on Laboratory Animal Care Committee of Stanford University (protocol #33691).

Sequencing for feeding experiment samples

DNA was extracted from swabs using the Qiagen PowerSoil Pro Kit, adapted for use with dry swabs. Swabs were included through the addition of solution CD2, at which point swabs were removed and the protocol continued per manufacturer instructions. Extracted DNA was sent to the University of Oregon Genomics and Cell Characterization Core Facility for library preparation and sequencing. The 16S rRNA samples were prepared using the LabCyte liquid handler in 384 well plates by combining 5 μL 2x Q5 Hot Start, 4.4 μL nuclease free water, 100 nL of forward (515F 5'-GTGYCAGCMGCCGCGGTAA-3') and reverse (806R 5'-GGAC TACNVGGGTWTCTAAT-3') primers with unique barcodes for demultiplexing, and 400 nL of sample or blank.[54] PCR conditions were as follows: 98 °C for 30 s, 35 cycles of 98 °C for 10 s, 61 °C for 20s, 72 °C for 20 s, followed by a final elongation period of 2 minutes at 72 °C. ITS samples were prepared by combining 12.5 μL master mix, 6.2 μL forward primer (ITS1F-kabir 5'-CTTGGTCATT TAGAGGAAGTAA-3') at 2.5 uM, 1.25 μL reverse primer (ITS2R-kabir 5'-GCTGCGTTCTTCATCGATGC-3') at 10 μM and 5 μL template or blank. PCR parameters were as follows: 30 s at 98 °C, followed by 35 cycles of 30s at 98 °C, 30 s at 60 °C, 30 s at 68 °C, and a final elongation step of 7 min at 68 °C. For both 16S rRNA and ITS, samples were bead cleaned twice with 0.8x beads and were eluted in Buffer EB (Qiagen). Libraries were measured with Qubit and pooled in equimolar amounts. Pooled libraries were quantified by qPCR and sequenced on two lanes (380 samples per lane) in a 2x300 configuration on Illumina MiSeq v3 with 25% PhiX.

Feeding experiment alkaloid quantification

At the conclusion of the laboratory feeding experiment, frogs were anesthetized with benzocaine application to the ventral side and euthanized via cervical transections. Dorsal skins were removed and placed in Trizol (Invitrogen) and immediately homogenized in BeadBug tubes for 6 cycles of 30s at speed 5 with a 1 min delay between cycles, then stored at -80 °C until used for alkaloid extractions. Homogenized samples were thawed and weighed to account for size of skin used for analysis. The liquid (~1 mL) was removed from the BeadBug tubes and transferred to new tubes with 150 μL of chloroform. Tubes were shaken for 15 s, then left at room temperature for 3 min. Samples were then spun down at 15682 rcf for 15 min at 4 °C. The top layer was removed and 300 μL of 100% ethanol was added to the remaining organic phase, then mixed by inverting 10 times and allowed to settle for 3 min at room temperature. The samples were centrifuged at 2000 rcf for 5 min at 4 °C to pellet the DNA, then 300 μL of the supernatant was transferred to a new tube along with 900 μL of acetone. The samples were mixed by inversion for 10-15 s, then incubated for 10 min at room temperature. The samples were then centrifuged for 10 min at top speed at 4 °C to pellet the protein precipitate, then 1 mL of the supernatant was removed and placed into glass vials. The supernatant was filtered through a 0.1 μM filter, then dried down under N_2 gas and reconstituted in 270 μL methanol with 30 μL of a 700 μM nicotine solution to be used as an internal standard. The samples were centrifuged at 5000 rcf for 5 min to pellet any remaining particulate, and 100 μL was removed and placed into autosampler vials for LC/MS analysis. Samples were diluted 1:5 to fit within the dynamic range of the instrument. The samples were analyzed by ESI-MS on the Waters Acquity UPLC and Thermo Exploris 240 BioPharma orbitrap mass spectrometer. A Sequant zic-HILIC 3.5u 100 x 2.1 mm LC column was used with a flow rate of 0.2 mL/min with an injection volume of 5 μL. The solvents used were 5 mM ammonium acetate and 0.1% formic acid in water (Solvent A) and 0.1% formic acid in acetonitrile (Solvent B). The solvents were used with the following gradient: 10% A, 90% B for 0.5 min, ramped to 20% B in 14 min and held for 2 min. Full Scan MS and targeted Full Scan MS2 data were acquired: FullMS mass range 100-1000 with resolution 120,000; FullMS2 of m/z 140.1434 (DHQ) and FullMS2 of m/z 163.123 (nicotine ISTD) isolation window=2, microscans=1, with fixed absolute HCD collision energy of 20 and resolution 15,000. To calculate the adjusted DHQ amounts, the area under the curve (AUC) for DHQ was divided by the AUC for nicotine, then by the calculated skin weight for each sample.

Please cite this article in press as: Caty et al., Alkaloids are associated with increased microbial diversity and metabolic function in poison frogs, Current Biology (2024), https://doi.org/10.1016/j.cub.2024.10.069

Metagenomics

Extracted DNA from the feeding experiment and the field samples were used to generate metagenomic libraries. Five samples each from wild *Allobates femoralis* and *Oophaga sylvatica* were used, as well as 5 samples from the pre (day 12) and post (day 19) of the feeding experiments were used to generate metagenomic libraries with the NexteraXT library prep kit (Illumina). Metagenomic libraries with concentrations above 5 ng/uL were submitted for sequencing, which included samples from wild *A. femoralis* (N=5), wild *O. sylvatica* (N=5), *O. sylvatica* DHQ pre (N= 4), *O. sylvatica* DHQ post (N=5), *O. sylvatica* control pre (N=3), *O. sylvatica* control post (N=2), *A. femoralis* DHQ pre (N=5), *A. femoralis* DHQ post (N=4), *A. femoralis* control pre (N=5), and *A. femoralis* control post (N= 5). These libraries were pooled into two groups at equimolar concentrations and run on two 2x150 HiSeq lanes with 5% PhiX spike in.

Microbial isolate library characterization

When colonies were large enough to be picked (ranging from about 12–168 hours), they were isolated three times by re-streaking onto new plates of the same media type. A single colony from the third plate was used for both isolate identification and glycerol stock production. To identify colonies, samples were prepared for full length 16S rRNA sequencing or ITS region 1 Sanger sequencing as follows. Individual colonies were placed into 10 μL of sterile water and 1 μL of this input was used in a PCR reaction with 1 μL each of forward primer 27F (5'-AGAGTTTGATCMTGGCTCAG-3') and reverse primer 1492R (5'-TACGGYTACCTTGTTAYGACTT-3')[44] for 16S rRNA or forward primer ITS4 (5'-TCCTCCGCTTATTGATATGC-3') and reverse primer gITS7 (5'-GTGARTATCGARTCTTTG-3) for ITS,[45,46] 12.5 μL of OneTaq polymerase (New England Biolabs) and 9 μL water. Bacterial PCR parameters were as follows: denaturation for 30 s at 94 °C followed by 30 cycles of denaturation for 15 s at 94 °C, annealing for 30 s at 55 °C and extension for 2 min at 65 °C, then a final extension period of 5 min at 65 °C. Fungal PCR parameters were as follows: denaturation for 30 s at 94 °C followed by 30 cycles of denaturation for 15 s at 94 °C, annealing for 30 s at 55 °C and extension for 2 min at 68 °C, then a final extension period of 5 min at 68 °C. Colony amplification was confirmed with gel electrophoresis, after which samples were cleaned with the E.Z.N.A Cycle Pure Kit (Omega). If no amplification occurred, DNA was extracted from colonies using the Qiagen Blood and Tissue Kit adapted for samples from gram positive bacteria. Fungal samples that could not be lysed with either of the above methods were regrown in liquid media, pelleted, and treated with 20 μL of water and 4 μL of a 1:5 dilution of the stock solution of zymolyase (Zymo Research) prior to the first step of the Blood and Tissue Extraction. Cleaned DNA samples were submitted to Azenta for Sanger sequencing. Forward and reverse reads were aligned using the Geneious Alignment in Geneious Prime with the following parameters: global alignment with free end gaps, 65% similarity (5.0/-4.0) cost matrix, gap open penalty 12, gap extension penalty 3. The aligned sequences were BLASTed with Megablast on Geneious Prime to either the 16S ribosomal RNA database for bacteria or the nucleotide collection nr/nt for fungi. Glycerol stocks were made by combining equal parts of a sterile-filtered 50% glycerol and water solution with cultures grown overnight in liquid media matching the initial isolation media. Glycerol stocks were maintained in duplicate at -80 °C for downstream use.

Isotope labeling nanoSIMS experiments

We performed two isotope tracing experiments with nanoSIMS to test whether any microbes on the skins of *O. sylvatica* may be able to metabolize the alkaloid DHQ. In the first experiment, we swabbed the skin of *O. sylvatica* and incubated those swabs in M9 minimal media with 0.2% w/v of a custom ^{13}C labeled version of DHQ (Cambridge Isotope Laboratories) for 48 hours to determine whether microbial cells incorporated with ^{13}C into their biomass. At the end of 48 hours, paraformaldehyde (PFA) was added to a final concentration of 4% to fix the cells. The number of cells collected from a swab was too low to use as a killed control, so instead we grew two bacterial isolates (*Providencia* sp. and *Serratia* sp.) in M9 minimal media with glucose, fixed those cells with PFA for 2 hours, then rinsed and resuspended the cells in PBS and incubated those cells with the same DHQ media to account for the stickiness of DHQ to fixed cells. For the second experiment, we used the same two isolates, which were cultured from *Oophaga sylvatica* skins using M9 media with DHQ as the sole carbon source, for a reverse labeling isotope tracing analysis with nanoSIMS to test for metabolism of DHQ. The idea was to incubate ^{13}C-labeled cells in unlabeled DHQ and examine the dilution of isotope over time, which would be consistent with utilization of DHQ carbon. Isolates were grown from glycerol stocks in M9 minimal media with glucose overnight. In an attempt to fully label the cells with ^{13}C, 100 μL of each isolate was transferred from the unlabeled glucose M9 media to 5 mL of M9 media with 50% ^{13}C glucose (99% ^{13}C, Cambridge Isotope Laboratory) and 50% natural abundance glucose and allowed to grow overnight at room temperature, shaking at 210 rpm. Then 100 μL of each isolate was transferred to 5 mL of 99% ^{13}C glucose twice. After the second round of growth in 99% ^{13}C glucose, the isolates were spun down for 15 min at 3000 rcf to pellet the cells, then washed twice with PBS to remove residual glucose. After the second wash, the isolates were resuspended in PBS and divided amongst one of three treatments: experimental, methanol control, or kill control. In the experimental condition, 100 μL of resuspended cells were added to M9 media with decahydroquinoline (DHQ; $C_9H_{17}N$; natural carbon abundance: 99.93% ^{12}C, 1.07% ^{13}C) dissolved in methanol and $^{15}NH_4Cl$. In the methanol control, the isolates were added to M9 media with an equivalent amount of methanol and $^{15}NH_4Cl$ as used in the experimental treatment, but with no DHQ. For the kill control, 100 μL of the resuspended cells were fixed in paraformaldehyde (PFA) at a final concentration of 4% for two hours, then washed once with PBS and added to M9 media with DHQ and $^{15}NH_4Cl$, as in the experimental treatment (Figure 4C). In addition to these treatments, a no-addition control was generated to determine the ^{13}C baseline for the isolates prepared in natural abundance glucose and subsequently transferred to M9 media with DHQ dissolved in methanol with unlabeled NH_4Cl. Initial time point (t0) samples were collected immediately after inoculation. At 48 hours (t48), the unfixed samples (experimental, methanol control and no addition control) were fixed with PFA

Please cite this article in press as: Caty et al., Alkaloids are associated with increased microbial diversity and metabolic function in poison frogs, Current Biology (2024), https://doi.org/10.1016/j.cub.2024.10.069

at a final concentration of 4% for two hours, then washed once and resuspended in 1 mL of PBS. The kill control was spun down at 3000 rcf for 15 min to pellet the cells, then the supernatant was removed and the pellet was resuspended in PBS.

Samples from both experiments were prepared for nanoSIMS following previously established protocols.[55] Briefly, the samples were filtered onto 0.2 μM pore white polycarbonate membrane filters (Whatman Nucleopore, GE Healthcare Life Sciences, Pittsburg, PA). Samples from swabs and the initial time points (t0) were undiluted while t48 samples were diluted 1:10 to adjust for higher cell concentration. Filters were rinsed with milliQ water, then left to dry completely. After drying, sterile scissors were used to cut slices of each filter and adhered to an analysis bullet using conductive tabs and sputter coated with ~5 nm of gold. Isotope imaging was performed with a Cameca NanoSIMS 50 at Lawrence Livermore National Laboratory. A primary 133 CS + ion beam (2 pA, 150 nm diameter, 16 keV) was rastered over a 25 x 25 um analysis area with 256 x 256 pixels and a dwell time of 1 ms/pixel for 25–30 cycles. Prior to the analysis, areas were sputtered with 90 pA of Cs+ current to reach sputter equilibrium. Secondary ion images were simultaneously collected for $^{12}C_2^-$, $^{12}C^{13}C^-$, $^{12}C^{14}N^-$, $^{12}C^{15}N^-$ and $^{32}S^-$ on individual electron multipliers in pulse counting mode, as described by Pett-Ridge and Weber.[56]

QUANTIFICATION AND STATISTICAL ANALYSIS

16S rRNA and ITS amplicon sequencing analysis

Both the field sample and feeding experiment 16S rRNA and ITS datasets were cleaned and processed with the R package dada2 (version 1.26.0).[57] The 16S rRNA sequences from the field were filtered and trimmed based on quality and to remove primers (trimLeft=c(20,20), maxN=0, maxEE=c(2,2), trunQ=2). Since ITS reads are more variable in length and there is a higher likelihood of reverse primers being sequenced in a forward read, all orientations of all primers were trimmed from sequences using cutadapt (version 4.2, Python version 3.7),[58] then samples were filtered and trimmed further based on quality and length using dada2 (maxN= 0, maxEE=c(4,4), truncQ=2, minLen=75). The 16S rRNA sequences from the feeding experiment were filtered and trimmed with the following parameters: truncLen=c(260, 200), maxN=0, trimLeft=c(6,0), maxEE=c(3,4), truncQ=2). The ITS sequences from the feeding experiment were filtered and trimmed with the following parameters: maxN=0, maxEE=c(2,2), truncQ=2, minLen=75. After filtering and trimming, 16S rRNA and ITS sequences were error corrected, denoised, dereplicated, merged with forward and reverse reads, and cleaned of chimeras, all using dada2. Taxonomy was assigned to 16S rRNA reads with the Silva NR99 version 138.1 dataset, and to ITS reads with the UNITE version 29.11.2022 database. Phylogenies were constructed using phangorn (version 2.11.1).[59] The amplicon sequence variants (ASVs) generated from dada2 were incorporated into phyloseq objects for additional data analysis (phyloseq version 1.42.0, Biostrings version 2.72.1).[60] As a conservative measure, any ASVs found in control sequencing reactions were removed from the datasets. For the 16S rRNA datasets, any ASVs with a phylum designation that was uncharacterized, "NA", or Eukaryotic, or a family designation of Mitochondria were removed from the datasets. For the ITS data, uncharacterized and "NA" phyla were removed. To account for differences in sampling depth, alpha diversity analyses were conducted with rarefied datasets. For 16S rRNA alpha diversity comparisons in the field samples, samples with fewer than 10,000 reads were excluded (average read depth=32,039), and then all samples were rarefied to the read number of the sample with the fewest reads. Because the number of reads were lower from the feeding experiment samples, samples from the feeding experiment with fewer than 5,000 reads were excluded (average read depth=32,625), and then all samples were rarefied down to the read number of the sample with the fewest reads to maintain as many samples as possible. For beta diversity-based analyses in all datasets, the samples were not rarefied, but any ASVs found in only one frog were removed and counts were converted into relative abundance. For beta diversity analyses in the field data, ASVs were agglomerated at the genus level to facilitate comparison across the disparate ASVs found across the poison frog species. All statistical analyses were performed in R (version 4.2.1). Faith's phylogenetic distance was calculated using picante (version 1.8.2).[61] Faith's phylogenetic distance is commonly used in other fungal studies, however it should be noted that there are limitations in its application to fungal data.[62] Bray-curtis dissimilarity and weighted unifrac distance were used for PERMANOVA analyses in vegan (version 2.6.4)[63] and posthoc pairwise testing with metagMisc (version 0.5.0). A phylogenetic tree containing each of the species from the field analyses was imported from Grant et al.[64] and parsed down to contain only the species of interest using the R packages ape (version 5.8)[65] and phylobase (version 0.8.12).[66] Geographic location data was imported as latitude and longitude coordinates for each collection site and converted to a distance matrix using the R package geosphere (version 1.5.18).[67] Mantel tests between distance matrices were performed with vegan (version 2.6.4) using ecodist (version 2.1.3),[68] as in Weinstein et al.[69] Dendrograms were generated with dendextend (version 1.17.1).[70] Differential abundance analyses were conducted with ANCOMBC (version 2.0.3)[23] and the associated packages TreeSummarizedExperiment (version 2.12.0),[71] mia (version 1.12.0),[72] and DT (version 0.33).[73] ANCOMBC is designed specifically for microbiome data to account for the unequal sample depths of individual samples and the biases inherent in sequencing efficiency across different microbial taxa. ANCOMBC uses Aitchison's methodology for false discovery rate correction, which enables higher power with fewer false positives than other differential abundance packages.[23] Identification of indicator taxa was performed with labdsv (version 2.1.0).[74] Associated heatmaps were generated with gplots (version 3.1.3.1).[75] The R packages tidyr (version 1.3.1),[76] dplyr (version 1.1.4),[77] and ggplot2 (version 3.5.1)[78] were used for data cleaning, manipulation, and visualization.

Metagenomics analysis

All data processing and analysis was performed in KBase.[79] Adapter sequences were removed using Cutadapt (v1.18),[58] then reads were trimmed and quality filtered using trimmomatic (v0.36)[80] with the following parameters: sliding window size=4, sliding window minimum quality=15, head crop length=10, leading and trailing minimum quality=3, minimum read length=36. Read quality was

Please cite this article in press as: Caty et al., Alkaloids are associated with increased microbial diversity and metabolic function in poison frogs, Current Biology (2024), https://doi.org/10.1016/j.cub.2024.10.069

confirmed with FastQC (v0.11.9).[81] Metagenomes were assembled both at the individual sample level and at the group level (*A. femoralis* field, *O. sylvatica* DHQ pre, etc.) using metaSPAdes (v3.15.3).[82] Metagenomes were annotated and summarized with DRAM (v0.1.2).[83] DRAM annotation categorizes genes into carbon utilization, transporters, energy, organic nitrogen, and miscellaneous. Given our interest in potential DHQ metabolism and processing, we focused on carbon and nitrogen metabolism, as well as transporters. Gene counts were adjusted for assembly quality by dividing gene counts by the total number of genes in an assembly. Individual frog level assemblies were used for statistical comparisons.

Quantification of microbial growth with an alkaloid

To measure the effect of the alkaloid DHQ on the growth of microbes isolated from *O. sylvatica*, individual isolates were grown in five concentrations of DHQ: 0%, 0.01% w/v, 0.1% w/v, 0.2% w/v and 1% w/v in 1% tryptone media. DHQ stocks were maintained in methanol, so methanol volumes were kept consistent across treatments and were below 1% of the total solution volume. Isolates were grown from glycerol stocks overnight at room temperature, shaking at 200 rpm in 1% tryptone then diluted to approximately 10^6 cells/mL as determined from OD600 readings. Then, 180 uL of media and 20 uL of the diluted isolate were added to each well. Plates were sealed with Breathe Easy (Sigma-Aldrich) membranes. Data was generated by measuring OD600 for four replicates of each condition at 5 min intervals until the strains reached stationary phase (48 hours for most strains; 96 hours with 8 min reads for slower growing strains) on a BioTek Epoch2 plate reader. Control wells were included for each DHQ concentration, and the average value for each control time point was subtracted from the experimental measurements for the respective treatments and time points. Growth curves were plotted using the plater package (version 1.0.4)[84] and growthcurver (version 0.3.1)[85] was used to fit curves and calculate the area under the curve. Areas under the curve were compared using ANOVA with a Tukey HSD post-hoc test. All statistical analyses were conducted in R (version 4.2.1). Isolates with at least one treatment with statistically higher AUC than the control (no DHQ) were characterized as enhanced. Otherwise, isolates were categorized as described.

NanoSIMS quantification

All images were processed using l'image (version 11-1-2021, Larry Nittler, Carnegie Institution of Washington). Ion image data were corrected for deadtime and image shift across cycles before producing $^{13}C^{12}C/^{12}C_2$ and $^{12}C^{15}N/^{12}C^{14}N$ ratio images. Regions of interest (ROIs) were autodetected in L'image using the $^{12}C^{14}N$ images. Ratios were averaged across cycles. Background corrections were performed for carbon ratios to adjust for differences across runs, and both carbon ratios and nitrogen ratios were converted to atom percent enrichment (APE) values based on the initial, pre-labeling (Ri) and final, post-labeling (Rf) ratios: $APE=[Rf/(Rf+1)-Ri/(Ri+1)]\cdot 100\%$[86]. Difference-in-differences analyses were performed in R (version 4.2.1) to compare the change in isotope enrichment between time 0 and 48 across the DHQ and methanol control treatments.